Polycyclic Aromatic Hydrocarbons and Redox Parameters in a Creosote-Contaminated Aquifer

Mark Elliott

Thesis submitted to the Faculty of Virginia Polytechnic Institute and State University in partial fulfillment of the requirements for the degree of

MASTER OF SCIENCE

in

ENVIRONMENTAL ENGINEERING

John T. Novak, Chair
Mark A. Widdowson
Duane Berry

February 5th, 2001
Blacksburg, Virginia

Keywords: Polycyclic Aromatic Hydrocarbons, Bioremediation, Creosote, Redox

Polycyclic Aromatic Hydrocarbons and Redox Parameters in a Creosote-Contaminated Aquifer

Mark Elliott

(ABSTRACT)

A groundwater monitoring study was conducted as part of a comprehensive program to remediate a former wood-preserving site that was contaminated with creosote. Twenty-five multi-level samplers (MLSs) were installed on-site and groundwater samples were collected and tested regularly between March 1998 and July 2000. Nearly one-thousand hybrid poplar trees were planted on-site in 1997 to help contain the groundwater plume and enhance phytoremediation. Ten polycyclic aromatic hydrocarbons (PAHs) were monitored along with several terminal electron acceptors (TEAs) and their reduced end products. The focus of the study was to determine the extent of natural biodegradation in the subsurface and assess the role of the poplar trees in site remediation.

Since monitoring began, considerable progress has been made remediating the site and the contaminant plume has been shrinking consistently. PAH levels in the groundwater and soil have been reduced and individual MLSs show consistently decreasing contamination.

At this point in the study it cannot be conclusively determined what impact the poplar trees are having on the progressing site remediation. However, there is a wealth of evidence indicating that natural biodegradation is playing a major role in site cleanup. Monitoring of TEAs indicates suggests that there are aerobic zones in the site aquifer, but that reduced conditions exist as well. Dissolved oxygen (DO) was found in many MLS ports, but other ports were devoid of both DO and nitrate and contained large quantities of aqueous Fe(II). Oxygen, nitrate and Fe(III) are being reduced on-site and data suggests that they are being used in the biological oxidation of PAHs.

Although laboratory studies document the oxidation of PAHs under sulfate-reducing conditions, high aqueous sulfate values were recorded throughout the site, regardless of the level of contamination. Several possible mechanisms are proposed to explain the

coexistence of high sulfate and PAHs in the site aquifer. The system may be redox-buffered by excess solid Fe(III) and Mn(III, IV) oxides. Also, dissimilatory sulfate-reducers are strict anaerobes and oxygen-rich rainwater may be toxic to them.

The presence of a layer of coal below land surface creates pyrite oxidation conditions similar to those encountered in conjunction with acid mine drainage. The MLSs most affected by the coal layer have less PAHs and DO, lower pH, and higher sulfate and Fe(II) levels than other wells.

The oxidation-reduction status of each MLS, based on oxygen, nitrate and Fe(II) measurements, appears to be closely related to the level of PAH contamination, suggesting that PAHs are the primary substrate being biologically oxidized in the site aquifer. These findings tend to support the general belief that the major limitation to natural biodegradation in subsurface environments is the delivery of adequate supplies of suitable TEAs to contaminated zones.

ACKNOWLEDGEMENTS

I would first like to thank Dr. John Novak for bringing me onto this project, providing guidance and direction, and sitting as my committee chairman. Thanks also go to Dr. Mark Widdowson for his involvement in my research, feedback on my thesis, and sitting on my committee. I would also like to thank Dr. Duane Berry for sitting on my committee.

Thanks go to Scott Crosswell for making my transition onto the project easier by training me in lab procedures and leaving the laboratory, data and project well-organized. I would also like to extend a special thanks to Sandra Robinson for her contribution to my work and her willingness to help with all aspects of my research.

Thanks also to Julie Petruska and Jody Smiley for help with lab equipment and analytical methods, and to Betty Wingate for scheduling meetings and defense.

Finally I would like to thank my family for their constant love, support and encouragement.

TABLE OF CONTENTS

CHAPTER 1. INTRODUCTION

Polycyclic aromatic hydrocarbons (PAHs) have been linked to toxic, carcinogenic, and mutagenic effects in humans and animals. Creosote, the contaminant of concern in this study, is composed of roughly 85% PAHs (Mueller et al., 1989). The U.S. Environmental Protection Agency (USEPA) lists sixteen PAHs as priority pollutants (Mihelcic and Luthy, 1988). Remediation of creosote contaminated sites, therefore, is of critical concern.

There are several options for the remediation of creosote-contaminated sites. However, creosote, like other hydrophobic dense non-aqueous phase liquids (DNAPLs), presents a formidable challenge. The chemical composition of creosote results in limited bioavailability and significant sorption to soil organic matter, especially for the higher molecular weight PAHs. Possible remediation methods include source removal and disposal, physical or hydrodynamic containment, pump-and-treat, phytoremediation, enhanced biodegradation, natural bioattenuation, and monitored natural attenuation.

This study will focus on the natural attenuation (NA) and phytoremediation occurring at our site and will consider the feasibility of monitored natural attenuation as a suitable remediation strategy. Monitored natural attenuation is a remediation strategy which relies on natural subsurface processes to clean up a contaminant. The goal of phytoremediation and natural attenuation studies should not be limited to simply demonstrating that degradation is occurring, but assessing whether it is occurring fast enough so that the risk to public health and the environment is acceptably low.

Of the mechanisms of NA, numerous studies have shown that the one mechanism that most affects the extent of the migration of the contaminant plume is biodegradation (Suarez and Rifai, 1999). The other mechanisms of NA, advection, dispersion, sorption, and volatilization, do not reduce the mass of the contaminant, but only change its concentration or location in the environment. However, sorption can be an effective means to remediating the heavier PAHs because of their tendency to irreversibly sorb to soil organic matter.

To evaluate on-site natural attenuation, electron acceptors are often measured in the aqueous phase to determine the level of microbial activity and subsurface oxidation-reduction (redox) status. Recently, investigators have devised ways of quantifying

mineral species integral to determining the subsurface redox state, as well (Kennedy et al., 1999).

Because the PAHs present in creosote are difficult to remove from soil and groundwater by other means, NA is thought to be an inexpensive alternative for remediation of subsurface soil and groundwater. In this study, groundwater was monitored for these ten PAHs: naphthalene, acenaphthylene, acenaphthene, fluorene, phenanthrene, anthracene, fluoranthene, pyrene, chrysene, and benzo(b)fluoranthene. Inorganic parameters monitored in groundwater include dissolved oxygen (DO), nitrate, nitrite, ferrous iron (Fe(II)), sulfate, pH, temperature, total sulfides, and chloride. Groundwater was sampled in March and June 1998; January, June, July and December 1999; and April 2000.

The objectives of this study were to determine the role of NA and biodegradation for the cleanup of creosote-contaminated sites and to study the relationships between inorganic parameters and PAHs in a bioactive subsurface. Inorganic parameters were chosen for analysis based on their importance in subsurface redox chemistry and the relative ease and low cost of analysis. DO, nitrate, and sulfate are important terminal electron acceptors (TEAs). Nitrite, sulfide, and Fe(II) are species are directly associated with the reduction of TEAs and can be used as measures of subsurface redox status.

Chapter 2 provides a literature review of the characteristics and microbial degradation of PAHs. The research methods are detailed in Chapter 3. Because this research was part of a larger, ongoing site remediation effort, the site history and remediation efforts to date are summarized in Chapter 4. Relationships and correlations in the inorganic redox parameters that we measured are then discussed (Chapter 5). This discussion is expanded in Chapter 6 to include PAH data and conclusions are drawn regarding the use of TEAs in the degradation of PAHs at our site. In Chapter 7 the major findings of this study are summarized.

CHAPTER 2. LITERATURE REVIEW

2.1 Introduction

When PAHs enter a subsurface environment, various physical, chemical and biological processes impact their fate and transport. Because PAHs constitute a variety of compounds with a broad range of properties, the individual compounds are impacted in different ways. Depending on the nature of the particular subsurface environment, the individual compounds may remain as a non-aqueous phase liquid (NAPL), desorb into the aqueous phase, be metabolized by microorganisms, taken up by plants, volatilize into the interstitial void spaces, or sorb onto soil or organic matter. For some PAHs, biodegradation may be the most likely mechanism of remediation. For other, more hydrophobic, PAHs, permanent binding to soil may account for their removal from groundwater.

A summary of some of the properties of the ten PAHs monitored in this study can be found in Table 2.1.

2.2 Characteristics of PAHs

Polycyclic aromatic hydrocarbons (PAHs) are composed of two or more fused benzene rings. PAHs pose an environmental threat primarily because of their toxicity, low volatility, resistance to microbial degradation, and ability to sorb to sediments (Coates et al., 1997). Some high molecular weight (HMW) PAHs have also been linked to carcinogenic and mutagenic effects in humans and animals (Malachova, 1999).

Creosote, the contaminant of concern in this study, contains roughly 85% PAHs by weight (Mueller et al., 1989). To properly consider remediation options for a creosote-contaminated site, one must understand the physical and chemical characteristics of creosote and its constituent PAHs.

The primary means of PAH remediation in the subsurface are biodegradation, volatilization, irreversible sorption, and direct plant uptake (Reilly et al., 1996). Bioremediation depends, to a large extent, on mass transfer of contaminants from the solid to the aqueous phase. Generally, only aqueous phase contaminants are considered bioavailable because only dissolved molecules are normally transported across cell

membranes (Zhang et al., 1998). Only low molecular weight (LMW) PAHs (those with two or three rings) have high enough vapor pressures for volatilization to be a significant remediation pathway. The HMW, more hydrophobic PAHs (those with four or more rings) are prone to irreversible sorption, while LMW PAHs are more likely to be directly taken up by roots.

Desorption from the solid phase is a critical factor in the degradability of PAHs. The tendency of a substance to sorb to soil can be quantified using the soil-water partition coefficient, which is useful in determining the probable subsurface fate of PAHs.

Because of the physical and chemical characteristics of LMW PAHs, such as naphthalene, they are often much easier to remediate than the higher MW PAHs found in creosote. LMW PAHs, such as naphthalene and methyl-naphthalenes, are relatively water soluble, but PAHs containing four or more rings are quite hydrophobic and insoluble. Therefore they usually remain bound to soil particles, sediments, or organic matter and are not transported with groundwater or surface water (Cerniglia and Heitkamp, 1989). Generally, the higher the molecular weight of a PAH, the more likely it is to sorb to soil organic matter (Table 2.1). This tendency to strongly sorb on particulate matter renders the HMW PAHs less available and thus less susceptible to bioremediation. If HMW PAHs are permanently sorbed to particles, the potential for off-site migration and adverse environmental effects is greatly reduced.

Generally, PAH biodegradation rates in natural sediments and water can be inversely related to the number of fused benzene rings in the compound (Cerniglia and Heitkamp, 1989). This is another factor facilitating the remediation of LMW PAHs to the possible exclusion of their heavier counterparts. LMW PAHs also have higher vapor pressures, making volatilization a significant remediation pathway (Table 2.1). High K_{oc} values have also been found to inhibit plant uptake, making lighter PAHs more amenable to direct phytoremediation (Schnoor et al., 1995).

Because lighter PAHs are more easily remediated, they can often be removed from creosote while the heavier ones remain. The selective removal of LMW PAHs results in a denser, more viscous, less soluble substance that is less likely to move off- site, but is also more difficult to remove from the subsurface. Rutherford et al. (1997) found that

Table 2.1: Chemical Characteristics of the Ten Monitored PAHs

PAH	Chemical Formula	Molecular Weight	Water Solubility mg/L	Soil-Water Partition Coefficient	Vapor Pressure (P^o) at 25 C (atm)
Naphthalene	$C_{10}H_8$	128.2	31.7	1300	1.05E-04
Acenaphthylene	$C_{12}H_8$	152	3.93	3814	
Acenaphthene	$C_{12}H_{10}$	154.2	3.93	2580	
Fluorene	$C_{13}H_{10}$	166.2	1.98	5835	7.94E-07
Phenanthrene	$C_{14}H_{10}$	178.2	1.29	23,000	1.62E-07
Anthracene	$C_{14}H_{10}$	178.2	0.073	26,000	7.94E-09
Fluoranthene	$C_{16}H_{10}$	202	0.275	19,000	1.23E-08
Pyrene	$C_{16}H_{10}$	202.3	0.135	63,000	7.24E-12
Chrysene	$C_{18}H_{12}$	228.2	0.006	420,108	
Benzo(b)fluoranthene	$C_{20}H_{12}$	252	0.0012	1,148,497	

Sources: Fetter (1993) and Schwarzenbach et al. (1993).

when LMW PAHs are selectively degraded the average molecular weight of the creosote increased from 10-36%.

2.3 Biodegradation

2.3.1 Aerobic Biodegradation

Fused polycyclic aromatic rings are very stable but studies have found many bacteria, fungi, and algae capable of metabolizing them (Cerniglia and Heitkamp, 1989). Numerous studies have documented that PAHs are biodegraded under aerobic conditions, but until recently, it was thought that most PAHs were recalcitrant under anaerobic conditions (Rockne, 1998). It is now known that PAHs can be degraded under a wide range of redox conditions (Section 2.3.2), but aerobic biodegradation is the fastest and most efficient means of PAH degradation.

When oxygen is available in the subsurface, it is much easier for unsubstituted aromatic rings to be cleaved and broken down. Under aerobic conditions, it is possible for PAHs to be completely degraded to CO_2 and H_2O (mineralization) or assimilated into microbial biomass (Cerniglia and Heitkamp, 1989).

It is preferable that oxygen be available to aid in the degradation of PAHs, but this is not always the case in sediments and the subsurface. Reoxygenation by diffusion from the atmosphere or infusion of oxygen-rich air into the subsurface is expensive, and inefficient, because of the relatively low water solubility of oxygen. However, recent evidence reveals that, under the right conditions, anaerobic biodegradation is a reasonable option for the remediation of PAHs.

2.3.2 Anaerobic Biodegradation

When a small plume of PAHs is introduced into the environment, a lack of oxygen is often the initial limiting factor to biodegradation. But as the LMW PAHs are remediated and the less readily degradable constituents are left, oxygen requirements decrease and groundwater flow can provide an adequate supply of oxygen (Brubaker et al., 1992).

However, in larger spills a redox series can develop (Stumm and Morgan, 1996). The convention is that electron acceptors are used in the following order: $O_2 > NO_3^- >$

Mn(IV) > Fe(III) > SO_4^{2-} > CO_2 (Kennedy et al., 1999). It is widely believed that these electron acceptors are depleted in the subsurface in a step-wise fashion, with one electron acceptor completely depleted before the next is used. The sequencing of these electron acceptors is thought to be determined by the amount of free energy (ΔG) that can be generated for the corresponding oxidation (Stumm and Morgan, 1996).

Although Mn(IV) reduction and methanogenesis are potential mechanisms of microbial remediation, they have not been widely investigated and no reports of PAH oxidation by either mechanism have been found. Thus, the following discussion will focus on the three TEAs for which PAH oxidation has been documented, namely, nitrate, Fe(III), and sulfate.

2.3.2.1 Nitrate Reduction

The reduction of nitrate to nitrite has been demonstrated by numerous investigators as a means of PAH degradation (Mihelcic and Luthy, 1988b; Rockne and Strand, 1998). The half-reaction is listed in Figure 2.1. As early as 1988, it was found that naphthalene and acenaphthene could be degraded under nitrate-excess conditions (Mihelcic and Luthy, 1988 a & b). However, their findings were not confirmed by other investigators for a number of years (Rockne et al., 1999).

Some researchers have demonstrated the biodegradation of even unsubstituted PAHs under denitrifying conditions after a period of acclimation. Mihelcic and Luthy (1988a) reported degradation rates of naphthalene and acenaphthene under denitrifying conditions that were within an order of magnitude of aerobic rates. More recently, Leduc et al. (1992) found that degradation rates of acenaphthylene, acenaphthene, fluorene, and anthracene in a denitrifying environment that were only 1.2 to 2 times slower than in an aerobic environment.

Nitrate has a higher aqueous solubility than oxygen, and can be added in the form of nitrate salts. Therefore, enhanced bioremediation may be more efficient if nitrate is added as the terminal electron acceptor instead of oxygen. However, according to Trepte (1999), Arvin et al. (1994) reported that nitrite can be toxic to nitrate reducing bacteria, limiting the effectiveness of nitrate reduction in the subsurface.

Figure 2.1: Redox Half-Reactions
Listed in order, Most to Least Efficient:

$\mathbf{O_2} + 4H^+ + 4e^- \leftrightarrow 2H_2O$

$\mathbf{NO_3^-} + 2H^+ + 2e^- \leftrightarrow \mathbf{NO_2^-} + H_2O$

$Fe^{3+} + e^- \leftrightarrow \mathbf{Fe^{2+}}$

$\mathbf{SO_4^{2-}} + 9H^+ + 8e^- \leftrightarrow \mathbf{HS^-} + 4H_2O$

$CO_2(g) + 9H^+ + 8e^- \leftrightarrow CH_4(g) + 2H_2O$

Note: Bold parameters are those monitored in this study

Source: Adapted from Stumm and Morgan, 1996.

Figure 2.2: Spatial Distribution of Redox Parameters

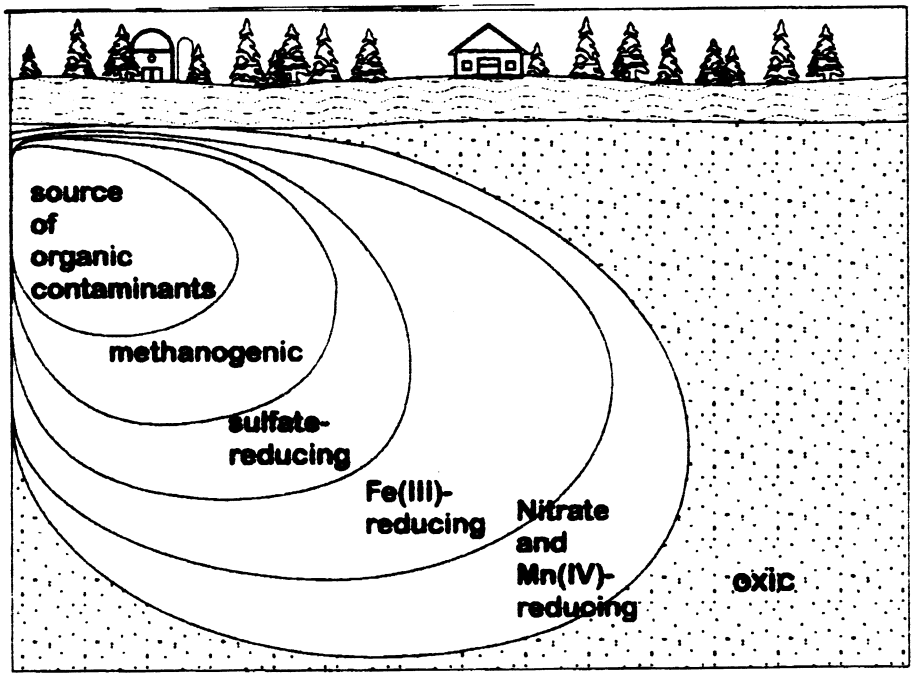

Source: Lovley, 1997.

2.3.2.2 Reduction of Ferric Iron Oxides

Ferric iron oxides are generally the most abundant potential electron acceptors in shallow aquifers (Lovley et al, 1994). However, they are fairly insoluble at the near neutral pH conditions that predominate in most groundwaters, and thus not highly accessible to microorganisms (Kennedy et al., 1999).

Fe(III) reduction in the subsurface is a slow process when compared with degradation under aerobic and denitrifying conditions. It was conventionally thought that the limiting factor was the slower metabolism of iron reducers. Recent studies, however, suggest that the limiting factor may be insolubility of Fe(III) oxides in the subsurface (Lovley et al., 1994; Trepte, 1999). Lovley et al. (1994) reported that when Fe(III) was made more available to subsurface microorganisms through the addition of chelating agents, degradation rates of benzene and toluene approached those observed in aerobic sediments. A later study found that adding Fe(III) ligands also enhanced the degradation of PAHs with two to six fused aromatic rings (Trepte, 1999). Studies such as these reveal that the Fe(III) oxides are available at nearly every hazardous waste site and that, through the addition of ligands and chelating agents, there is great potential for effective *in situ* remediation.

It is probably insufficient to monitor only aqueous parameters when trying to assess the degradation of Fe(III) oxides. Fe(II) is soluble in the aqueous phase, but has a strong tendency to react with sulfides to precipitate out of solution as insoluble iron sulfides (Kennedy et al., 1999). Methods for mineral analyses that can be used in conjunction with aqueous analyses are detailed in Kennedy et al (1999).

2.3.2.3 Sulfate Reduction

Until recently, sulfate reduction was not considered a significant remediation pathway because it was of insufficient energy to cleave fused aromatic rings (Cerniglia and Heitkamp, 1988). However, recent studies have provided evidence to the contrary.

Older literature indicates that there was previously some question whether sulfate reducing microorganisms were capable of degrading PAHs. Mihelcic and Luthy (1988a) reported that naphthalene and acenaphthalene showed no significant degradation under iron and sulfate-reducing conditions over periods of 50 and 70 days, respectively. But

recent evidence demonstrates that the capacity of microorganisms to biodegrade PAHs under sulfate-reducing conditions is dependent upon long-term exposure to the contaminants (Coates et al., 1997). Because most hazardous waste sites are contaminated for years before a remediation strategy is initiated, acclimating subsurface microorganisms to the contaminant should not be an obstacle to *in situ* remediation or field studies. However, it should be accounted for when studies are conducted under laboratory conditions.

Lovely et al. (1995) found that degradation of single-ring aromatics by sulfate-reducing organisms could be achieved in San Diego Bay sediments which had been exposed to PAHs for years. Degradation of PAHs under sulfate-reducing conditions was demonstrated on sediments from the same site (Coates et al., 1997). Rockne and Strand (1998) recently published data demonstrating the degradation of naphthalene and phenanthrene by sulfate-reducers, with nearly stoichiometric sulfide production in a study conducted on creosote-contaminated sediments from another site subjected to long-term contamination by PAHs.

When measuring indicators of sulfate-reduction, aqueous parameters may not be adequate. Fe(II) minerals can bind with HS^-, precipitating sulfides from solution. According to Kennedy et al. (1999), measuring aqueous sulfide parameters is not a reliable means of quantifying sulfate-reduction.

2.4 Phytoremediation

Direct phytoremediation involves direct plant uptake pathways of contaminants, usually through the roots. The contaminant is then metabolized by the plant and either incorporated into the plant biomass or volatilized through transpiration pathways.

The presence of roots in the subsurface can also enhance natural attenuation. Indirect phytoremediation, also called rhizosphere biodegradation or rhizofiltration, is the enhancement of microbial populations in the root zone that are capable of degrading the contaminants of interest. The rhizosphere, the subsurface soil just around the roots, is abundant in root exudates and readily degradable carbon-containing byproducts and is an environment where many microorganisms thrive.

2.5 PAH Behavior in the Subsurface

Though many laboratory studies have demonstrated the biodegradation of PAHs, there are many factors in the field that can inhibit the remediation of PAHs. Primary among these is the problem of bioavailability in the subsurface. Convention holds that for a PAH to be bioavailable, it must be present in the aqueous phase.

When a contaminant, such as creosote, is freshly added to a system, there is a fraction of the present PAHs which rapidly solubilize and can be degraded quickly. At this stage of degradation, microbial kinetics limits the degradation rate. Following this initial phase, however, is a phase of slower release in which desorption is the rate limiting step (Cornelissen et al., 1998). This is usually only the case for LMW PAHs, containing two to four rings, five and six ring PAHs are difficult to degrade even when they are found in the aqueous phase (Cornelissen et al., 1998).

After longer contact time between soil and contaminant, only the strongly sequestered contaminant remains, which is largely unavailable to bacteria. Tang et al. (1998) found that the sequestered contaminant, although it is only slowly available to microbes, may be accessible to higher organisms such as earthworms. Thus, some level of contaminant degradation occurs long after the initial pollution episode.

Since most hazardous waste sites have been exposed to the contaminant of concern for a long time, the initial, faster rates of biodegradation found with freshly-added contaminants are probably not representative of what will take place in the field. From a practical standpoint, any attempt to use enhanced bioremediation or natural attenuation to remediate a site contaminated with PAHs must take into account the final, slow phase of biodegradation (Cornelissen et al., 1998). However, the limited solubility of the heavier PAHs can result in irreversible sorption to minerals or soil organic matter, greatly reducing bioavailability and mobility and, thus, effectively remediating the site.

2.6 Conclusion

Most studies of PAH biodegradation have been conducted under controlled laboratory conditions. These studies have demonstrated that LMW PAHs can be oxidized under aerobic, nitrate-reducing, iron-reducing and sulfate-reducing conditions.

Lacking are field studies at PAH-contaminated sites that monitor inorganic redox parameters along with PAH compounds.

In this study, groundwater samples from the site were analyzed for both PAHs and various inorganic parameters that commonly serve as terminal electron acceptors or the reduced end-products from TEA processes. The concentrations of PAHs and inorganic species have been correlated at various locations around the site. This information was then used to provide insight on the state of *in situ* biodegradation as it is contributing to site remediation.

CHAPTER 3. METHODS AND MATERIALS

3.1 Experimental Approach

Determination of soil and groundwater contamination was necessary to ascertain the extent of creosote contamination of the site and the progress of remediation and natural attenuation. Depth-specific soil samples were taken at roughly twenty soil-borings, and depth-specific groundwater samples were taken at twenty-five multi-level samplers (MLSs) around the site. Sampling trips were taken in March 1998; January, June, July and December 1999; and April and July 2000.

3.2 Sample Collection

Soil samples were collected at depths between three and ten feet below ground surface (BGS) using a hand auger. Samples were then placed in mason jars or Ziploc bags and stored in coolers for transport back to Virginia Tech, where they were then stored at 4^{o}C until the extraction procedure was initiated.

Groundwater samples were collected at one foot intervals, at depths between 0.27 feet and 7.27 feet above bedrock, from MLSs installed by Virginia Tech. MLSs were color-coded to allow depth-specific groundwater sampling. Groundwater samples were stored in coolers on-site and placed in 4 ^{o}C storage upon return to Virginia Tech.

3.3 Field Procedures

Five groundwater parameters were measured in the field: ferrous iron (Fe(II)), dissolved oxygen (DO), pH, sulfide, and temperature.

Fe(II) was measured using a HACH DR/700 Colorimeter. Any noticeably turbid samples were filtered using 0.45 μm filters. Absorbance was read and converted to mg/L based on a standard curve constructed using ferrous sulfate crystals (Standard Methods, 1995).

DO was measured using a HACH Digital Titrator and following the Winkler Titration Method. The pH was measured with a HACH EC10 pH Probe. Temperature was measured with alcohol or mercury thermometers. However, because of occasional

delays between pumping the groundwater sample and measuring the temperature, the data was inconsistent and will not be discussed in this report.

Total sulfides were measured using a HACH DR/700 Colorimeter. All samples were filtered using 0.45 um filters. Because consistently low sulfide levels were detected for most of this study, sulfide data will only be discussed briefly in this report.

3.4 Laboratory Procedures

3.4.1 Groundwater Extraction Procedure

EPA methods for PAH extraction from groundwater samples were determined to be too expensive, time-consuming, and require too much solvent for our purposes. Therefore, the following extraction procedure was developed at Virginia Tech by Glendon Fetterolf and Dr. John T. Novak (Fetterolf 1998).

In the field, groundwater samples were collected in 40 mL amber vials, to prevent photodegradation, and refrigerated for transport back to the lab. Following storage at 4 ^{o}C, groundwater samples were removed from the refrigerator and the groundwater extraction procedure was initiated. A 37.7 mL volume of the groundwater sample was transferred to a 40 mL amber vial. It is important not to agitate the samples to ensure that no colloidal material or soil particles are transferred from the sample. After tightening the vial caps, 1.3 mL of Fisher Optima Grade methylene chloride (MeCl) was injected through the vial septa with a 1 mL gas-tight syringe. Each vial was vigorously hand-shaken for 90 seconds and the MeCl was allowed to settle for two minutes. Much of the MeCl settled to the bottom of the vial, but some remained as bubbles in solution or sitting on the surface of the water. By tapping the vial or shaking it lightly, more of the MeCl migrated to the bottom of the vial where the bubbles began to agglomerate. Tilting the vial to the side and tapping on the bottom enhanced agglomeration. Once one or two large bubbles of MeCl had formed at the bottom of the vial, the cap was removed and as much of the MeCl as possible was drawn into a 1.0 mL pipette. It is critical that water not be drawn into the pipette. The MeCl was then transferred to a GC vial. For some samples it was difficult to recover enough MeCl to fill the GC vial up to the recommended level for our Shimadzu AOC-20I Auto Injector. When this was the case,

we used National Scientific Micro-Sert Inserts as volume aids. GC vials were refrigerated for at least 4 hours before injection.

GC vials were labeled and run on a Shimadzu GC 14A gas chromatograph using a J&W Scientific DB5-MS fused silica capillary column and a flame ionization detector (FID). Helium was used as the carrier gas and the auxiliary gas and hydrogen was used as the fuel source for the FID. Sample injection volume was 2 μL.

Ten PAHs were measured in groudwater: naphthalene, acenaphthylene, acenaphthene, fluorene, phenanthrene, anthracene, fluoranthene, pyrene, chrysene, and benzo(b)fluoranthene.

3.4.2 Groundwater Anions

Samples to be run for anions were collected in the field in test tubes, capped, and placed in a cooler for the return trip to Virginia Tech. Upon return, they were placed in a 4^{o}C refrigerator and run as soon as possible.

Samples were run through a 0.45 μm filter before being run on a Dionex DX-300 Ion Chromatograph with an IonPac AS-14 column. Chloride, nitrite, nitrate, and sulfate were quantified.

3.4.3 Soil Boring Extraction Procedure

Since the soil boring extraction procedure is not essential to the data contained in this report, only a brief summary of the procedure will be reported here. A detailed account of the soil extraction procedure is presented elsewhere (Fetterolf, 1998).

Soil samples were air dried for four hours in a vent hood and then chopped into fine grains. Five grams of soil were placed in a 40 mL amber vial and 15 mL of MeCl was added. The sample vials were agitated on a rotating table for 36 to 48 hours, and then refrigerated for another 12 hours. Roughly one mL of MeCl was transferred to a 1.5 mL amber GC vial, and run on the Shimadzu GC 14A Gas Chromatograph detailed in Section 3.4.1.

Soil samples were tested on the gas chromatograph for the presence of six prominent PAHs: acenaphthene, fluorene, phenanthrene, fluoranthene, pyrene, and

chrysene. Groundwater samples used to quantify PAH contamination were stored in 40-mL amber vials until the extraction procedure was initiated.

CHAPTER 4. SITE ASSESSMENT AND REMEDIATION

4.1 Site History and Remediation Strategy

The site in the present study is located in the north-central part of Tennessee in the town of Oneida. In the early-1950s, Tennessee Railway Company began using the site as a railroad cross tie treatment facility, and it was in use for 16 years. In 1973, Tennessee Railway Company was purchased by Southern Railway Company (now known as Norfolk Southern Railway Company).

The tie treatment site included an above ground storage tank (AST), a treatment unit, a spur track, and a 6" pipe for transport of excess creosote to a nearby holding pond. Site runoff was collected in nearby sump pits, according to Norfolk Southern. The storage tank was situated on concrete footings and located roughly 100 feet north of Pine Creek.

In October 1990, a US Army Corps of Engineers team working nearby found evidence of creosote contamination in Pine Creek and reported it to the Tennessee Department of Health and the Environment (TDHE). TDHE monitoring of soil and groundwater revealed the presence of both BTEX and PAH components.

The strategy at this point was the prevention of further release of creosote into Pine Creek, and characterization of on-site contamination. Environmental Technology, Inc. (ETI) performed preliminary site assessment (PSA) in 1991. In 1993, an expanded site investigation (ESI) revealed that creosote was impacting Pine Creek sediments downstream of the site. Research has revealed that the accumulation of PAHs in sediments poses a danger to aquatic life (Sved et al., 1997).

In 1997, an investigation of the site identified the position of the former AST as well as other site details. Later that year, The Tennessee Department of Environment and Conservation approved a phytoremediation and intrinsic bioremediation remedial strategy for the site, as prepared by Geraghty and Miller, Inc.

In May 1997, approximately 1000 hybrid poplar trees were planted on the 1.7-acre site. Hybrid poplars were chosen for their ability to contain groundwater by root uptake and transpiration of volumes exceeding 50 gallons per tree per day when full-

grown (Matso, 1995). In addition to flow containment, poplars are also able to assist in contaminant cleanup via direct or indirect phytoremediation.

Both direct and indirect phytoremediation are likely occurring at our site but, at this point, evidence for the role of the poplars in remediation is limited. Monitoring of the site will continue for at least two more years, by which time the impact of phytoremediation should be resolved.

To help ensure that the contaminant plume did not migrate off-site and into the nearby Pine Creek, an interceptor trench was dug into the bedrock (Figure 4.1). The presence of the interceptor trench to contain flow made phytoremediation a feasible strategy as contamination could no longer move off-site. Contaminated groundwater is pumped out of the trench to a nearby separation tank where the contaminants are removed and the water is discharged to a sewer line.

The soil that was excavated when digging the interception trench was contaminated with creosote. That soil was spread over the site to a depth of roughly two feet. About 35% of the site was also covered in a layer of discarded coal from nearby rail yard. The coal was covered with the contaminated soil before the poplars were planted.

The layer of coal has introduced numerous obstacles to this investigation. Many trees have died because their roots have been unable to penetrate the coal layer to reach the groundwater table. Coal also causes positive interference when PAHs are measured in soil samples, so it is necessary to remove the bits of coal before extracting the sample. Initial sampling of soil and groundwater revealed that the most prevalent PAHs present in on-site soil were: acenaphthene, fluorene, phenanthrene, fluoranthene, pyrene, and chrysene. These six PAHs are monitored for all soil samples extracted and tested at Virginia Tech. In addition to these six, three more PAHs, naphthalene, acenaphthylene, and anthracene, were found in groundwater samples, and were monitored at Virginia Tech. Benzo(b)fluoranthene, as a refractory, largely insoluble PAH, was also monitored in groundwater samples as an indicator of extreme contamination. Extraction procedures were developed for PAHs in both soil and groundwater (Section 3.4).

4.2 Progress of Remediation Efforts to Date

Evaluation of remediation efforts so far can be based upon contaminant concentration trends in groundwater samples and soil samples from late 1997 to early 2000. A network of groundwater monitoring wells and multi-level samplers was installed throughout the site to monitor plume location and concentration, and inorganic parameters that would provide insight into the status of natural bioattenuation in the subsurface. Soil samples were also taken with a hand auger and monitored for relevant PAHs.

4.2.1 Groundwater Contamination

Figure 4.2 shows the distribution of PAHs in the contaminant plume at depths between 3 to 8 feet above bedrock in March 1998, January 1999, and December 1999. Total PAH levels were averaged over all samples between 3 and 8 feet above bedrock.

It appears from the figure that the plume is shrinking in size. The effect is especially pronounced toward the southwest corner of the site near the railroad tracks. The concentration data for the northeast corner of the plume is not included in Figure 4.2 because the small number of samples collected in that area made the data unreliable. Closer to bedrock the data was also unreliable, particularly in the most contaminated regions of the site. ML-7 and ML-11 would often pump free-product, making an accurate measure of the concentration of PAHs in groundwater impossible.

It is important to note that, in September 1998, what may have been a source of creosote was removed just up gradient of ML-2 and ML-3. The hole was then back-filled with gravel, allowing more oxygen-rich groundwater to reach Transect 1. Some of the reduction in PAH concentrations over Transect 1 is likely attributable to increased dilution and dispersion of contaminants with the increased groundwater flow. However, there is much evidence that natural bioattenuation plays an important role in remediating this area of the site (Chapter 6).

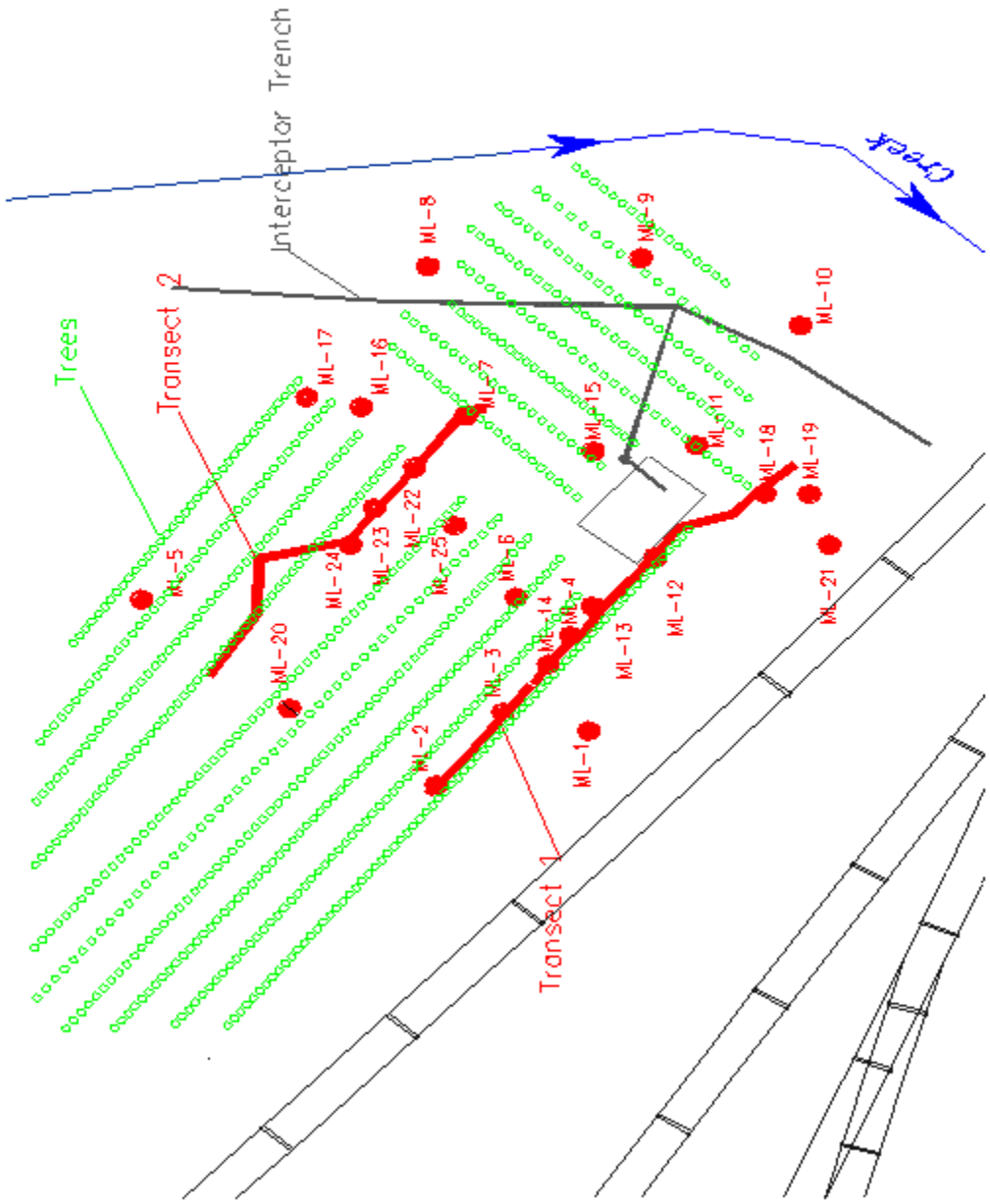

Figure 4.1: Site Map with Multi-level Samplers (MLSs) and Transects

March 1998

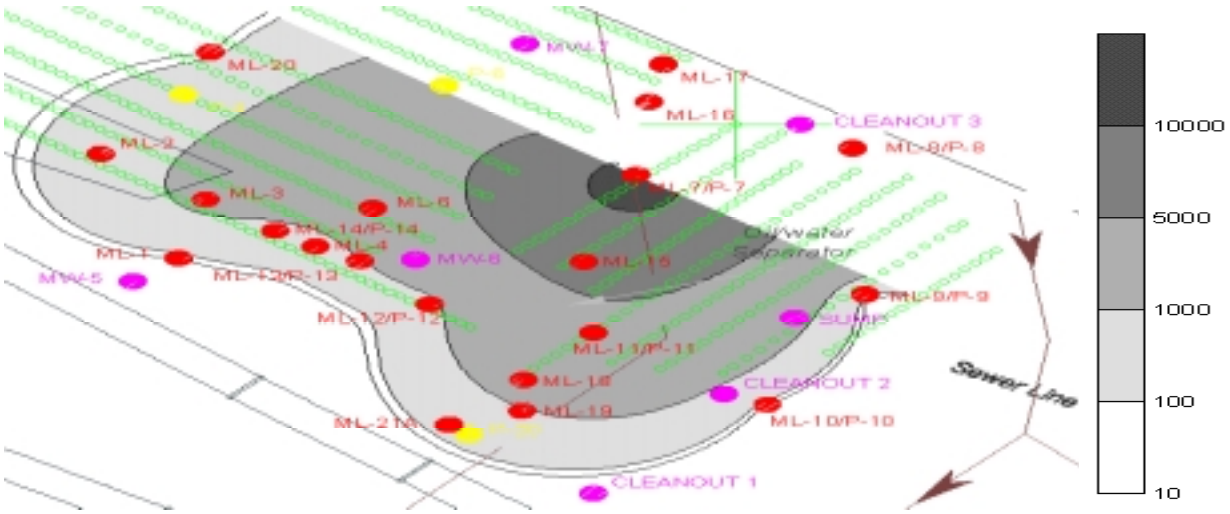

January 1999

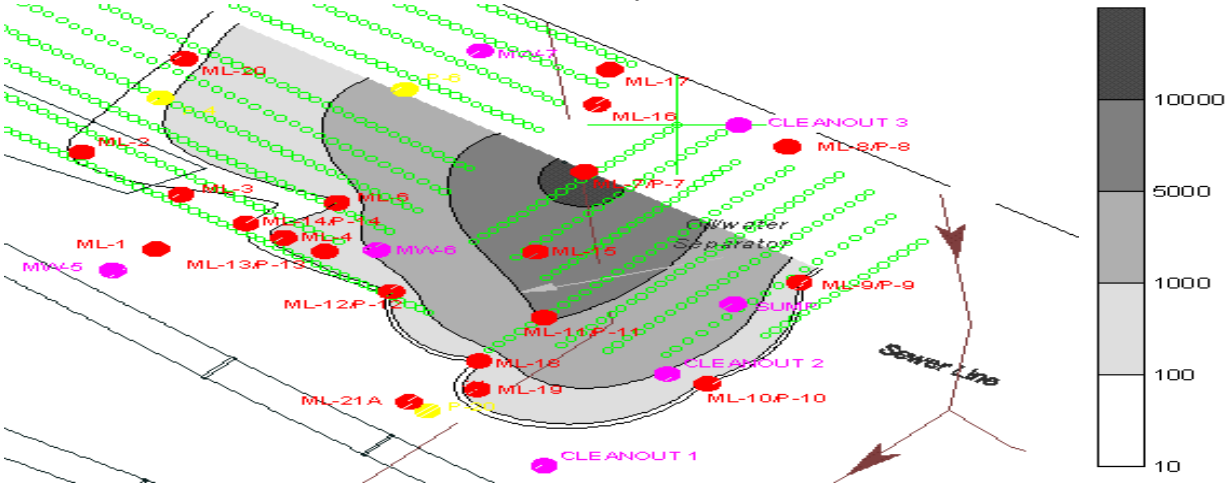

July 1999

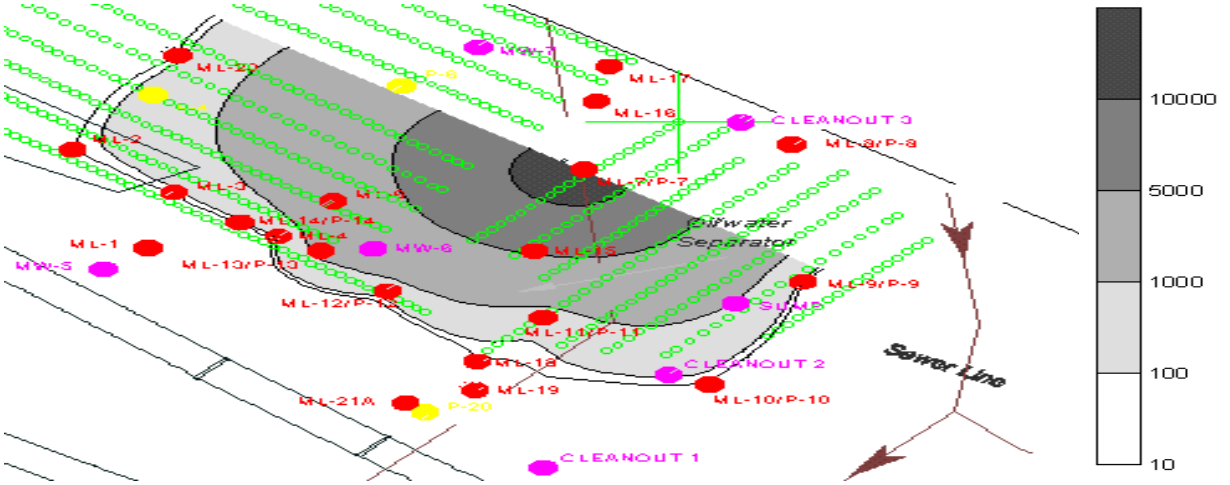

December 1999

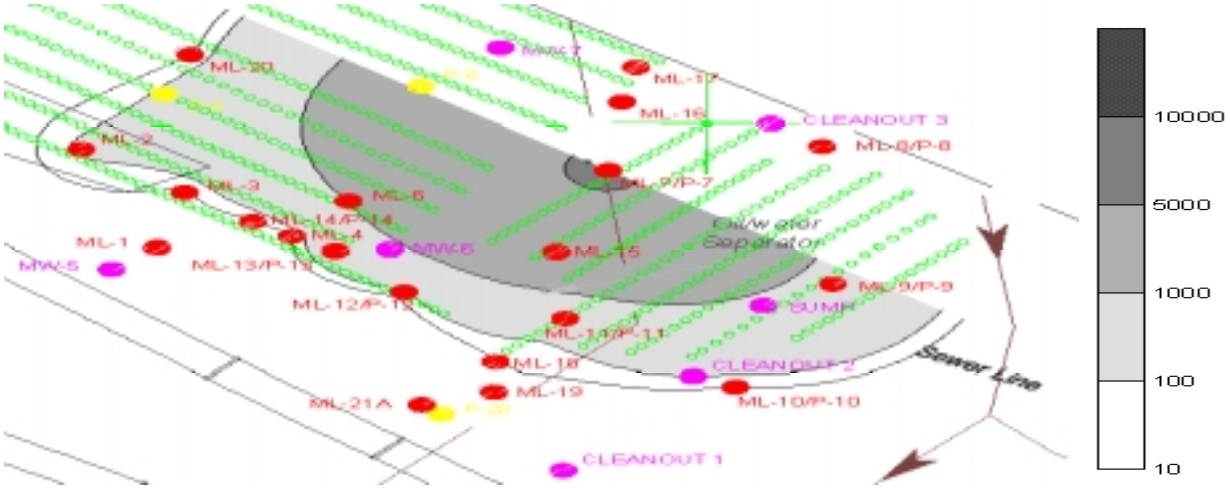

April 2000

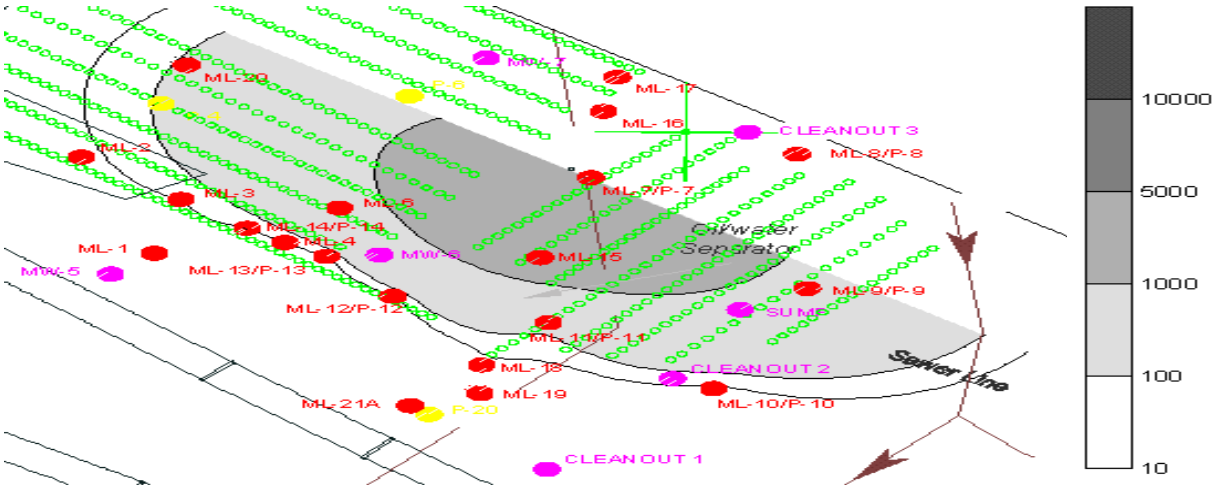

FIGURE 4.2: Average groundwater PAH concentrations (µg/L) for MLS ports between 3 and 8 feet above bedrock. (First-March 1998, Second-January 1999, Third-July 1999, Fourth-December 1999, Last-April 2000).

The groundwater transect (Transect 1 in Figure 4.1) that bisects the site provides valuable information on the movement of the plume. Levels of contamination are decreasing in on-site groundwater, as illustrated in Figures 4.3, 4.4 and 4.5. Naphthalene values in groundwater over time for Transect 1 reveal a decrease in the concentration of two-ring PAHs from March 1998 through December 1999 (Figure 4.3). Figures 4.4 and 4.5 show trends in the concentration of the monitored 3-ring and 4-ring PAHs, respectively. Note the different scales in the figures.

It appears from the three figures that the 2-ring and 4-ring PAHs have been remediated to a greater degree than the 3-ring species. Lighter PAHs are generally less recalcitrant and more easily cleaned-up than heavier PAHs, so the progress that has been made in remediating naphthalene is not surprising. The decrease in 4-ring PAHs may seem unexpected, but keep in mind that groundwater concentrations are displayed in Figure 4.5. It is likely that most of the 4-ring PAHs were sorbed to soil organic matter at some point and, thus, were not in the groundwater when these later samples were taken.

Because light PAHs are easier to remediate than heavier PAHs (Section 2.2), it was hypothesized that the fraction of heavier PAHs would increase with time. However, such effects were investigated in both soil and groundwater and there is no evidence that they are occurring at this point in the study. When in the presence of structurally similar compounds, the solubility of some hydrophobic, recalcitrant molecules can increase, making them more bioavailable. These multiple solute, or co-solvency, effects may be responsible for some of the remediation of heavier PAHs that we have seen on-site.

Figures 4.6 and 4.7 show the change in total PAH concentration with depth for three individual MLSs. The decrease in total PAHs in ML-3 is most striking because of its consistency over the four sampling times. Concentration profiles of ML-4 and ML-12 reveal similar downward trends (Figures 4.6 and 4.7). All three of these wells are in Transect 1 and the findings are consistent with the changes in the groundwater plume illustrated in Figure 4.2. The log-scale plots of these three wells are provided to better illustrate the trends at lower concentrations. Decreases in PAH concentrations in the shallow sampler ports may reveal the impact of the poplar roots reaching the groundwater table and contributing to cleanup via direct or indirect phytoremediation.

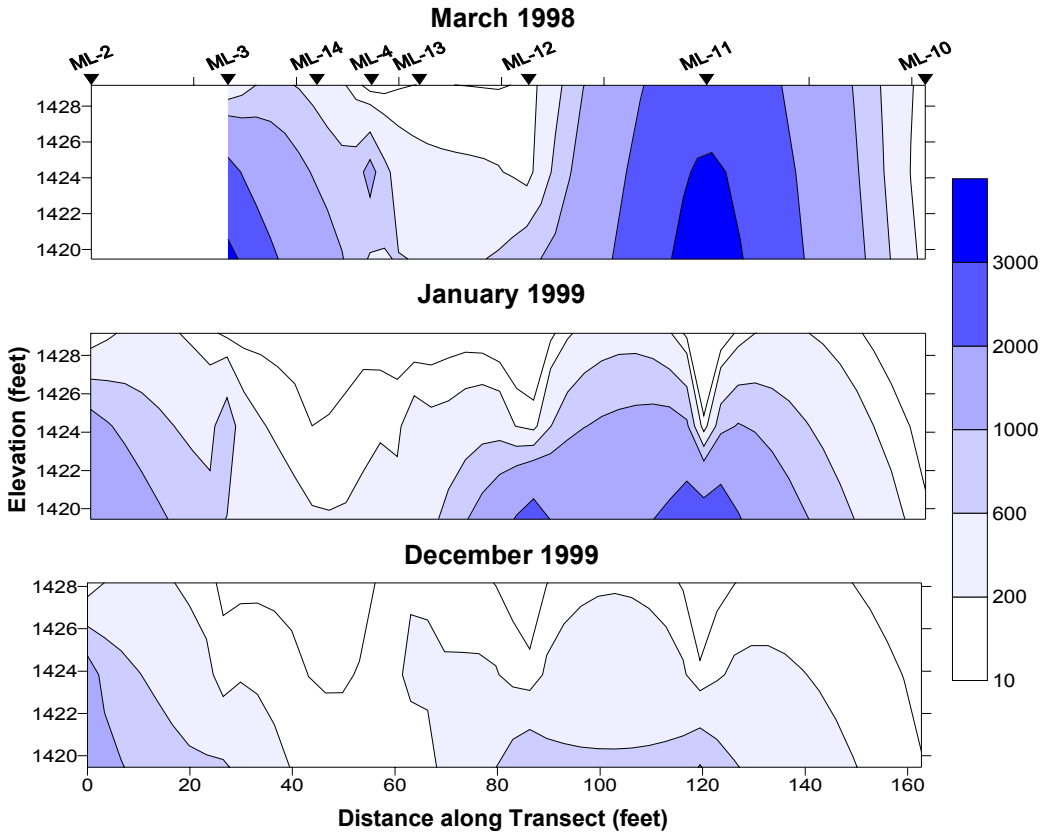

Figure 4.3: Changes in Groundwater Naphthalene Concentration (µg/L) over Time for Transect 1.

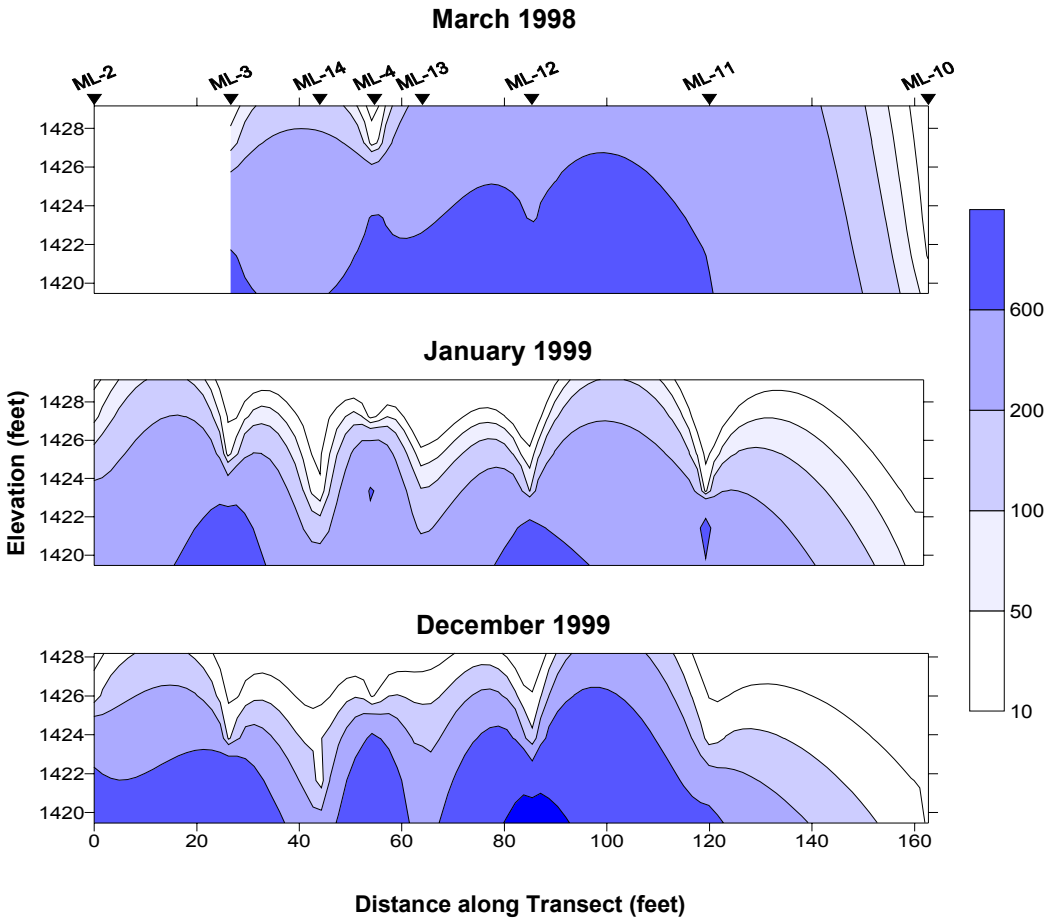

Figure 4.4: Changes in the Groundwater Concentration (µg/L) of Monitored 3-Ring PAHs (Acenaphthylene, Acenaphthene, Fluorene, Anthracene, Phenanthrene) over Time for Transect 1.

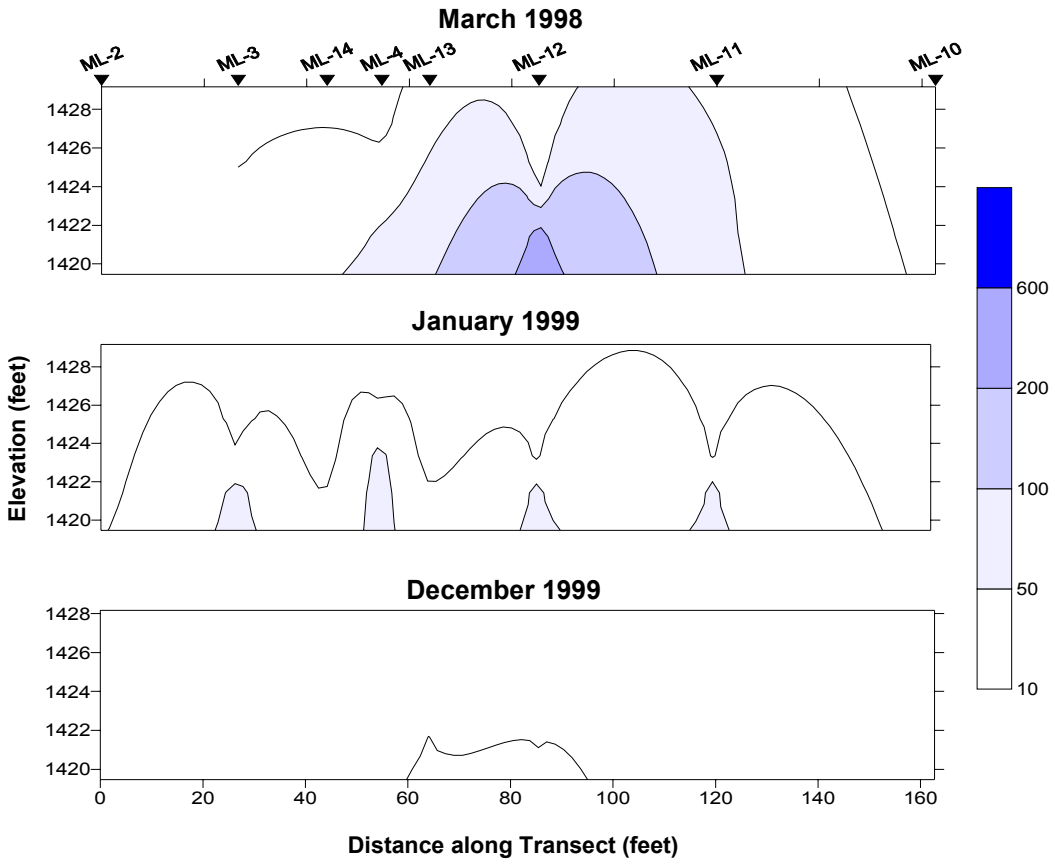

Figure 4.5: Changes in the Groundwater Concentration (µg/L) of Monitored 4-Ring PAHs (Fluoranthene, Pyrene, Chrysene) over Time for Transect 1.

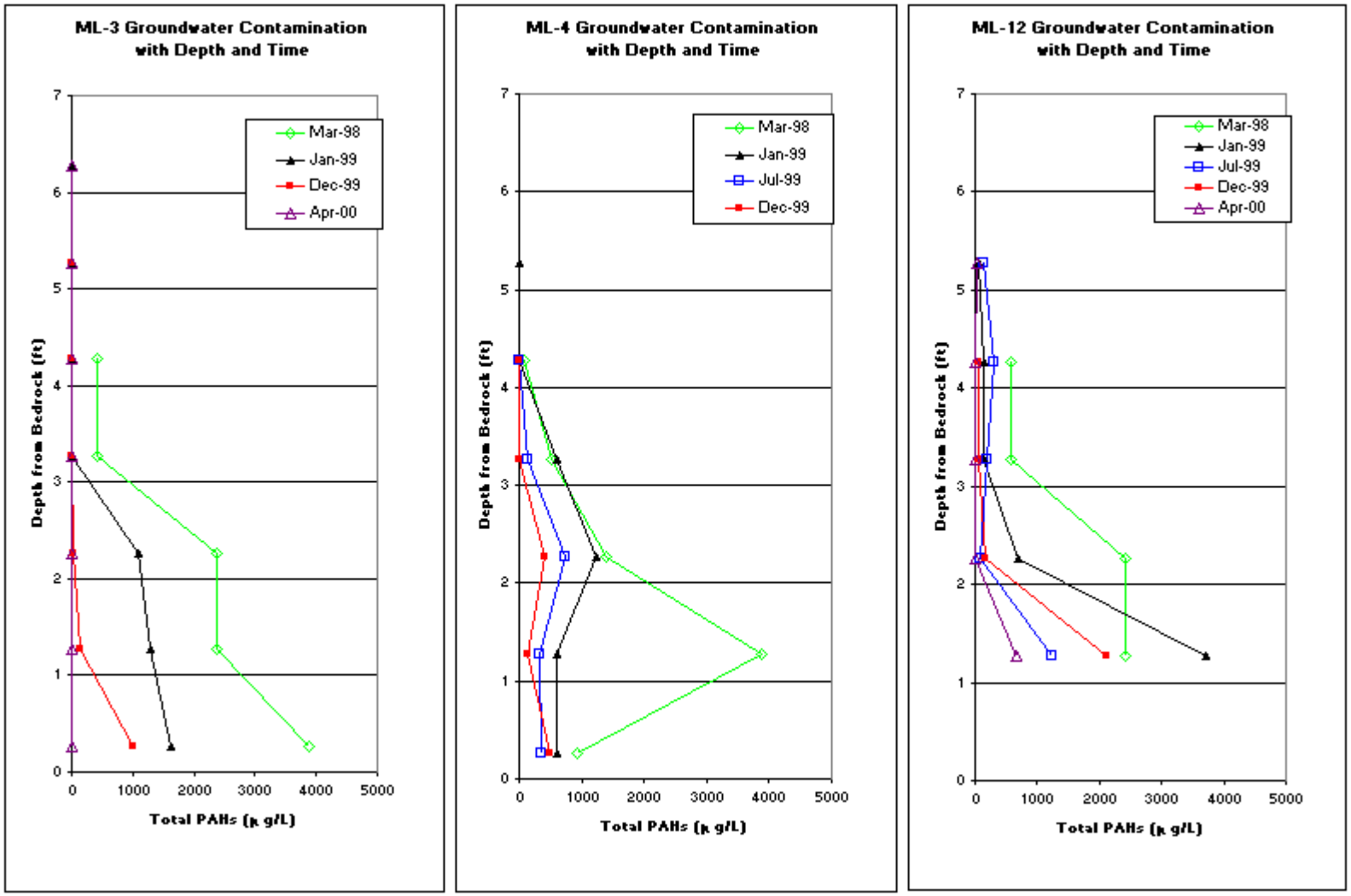

Figure 4.6: Change in Total PAH Concentration (µg/L) with Depth and Time for ML-3, 4 and 12.

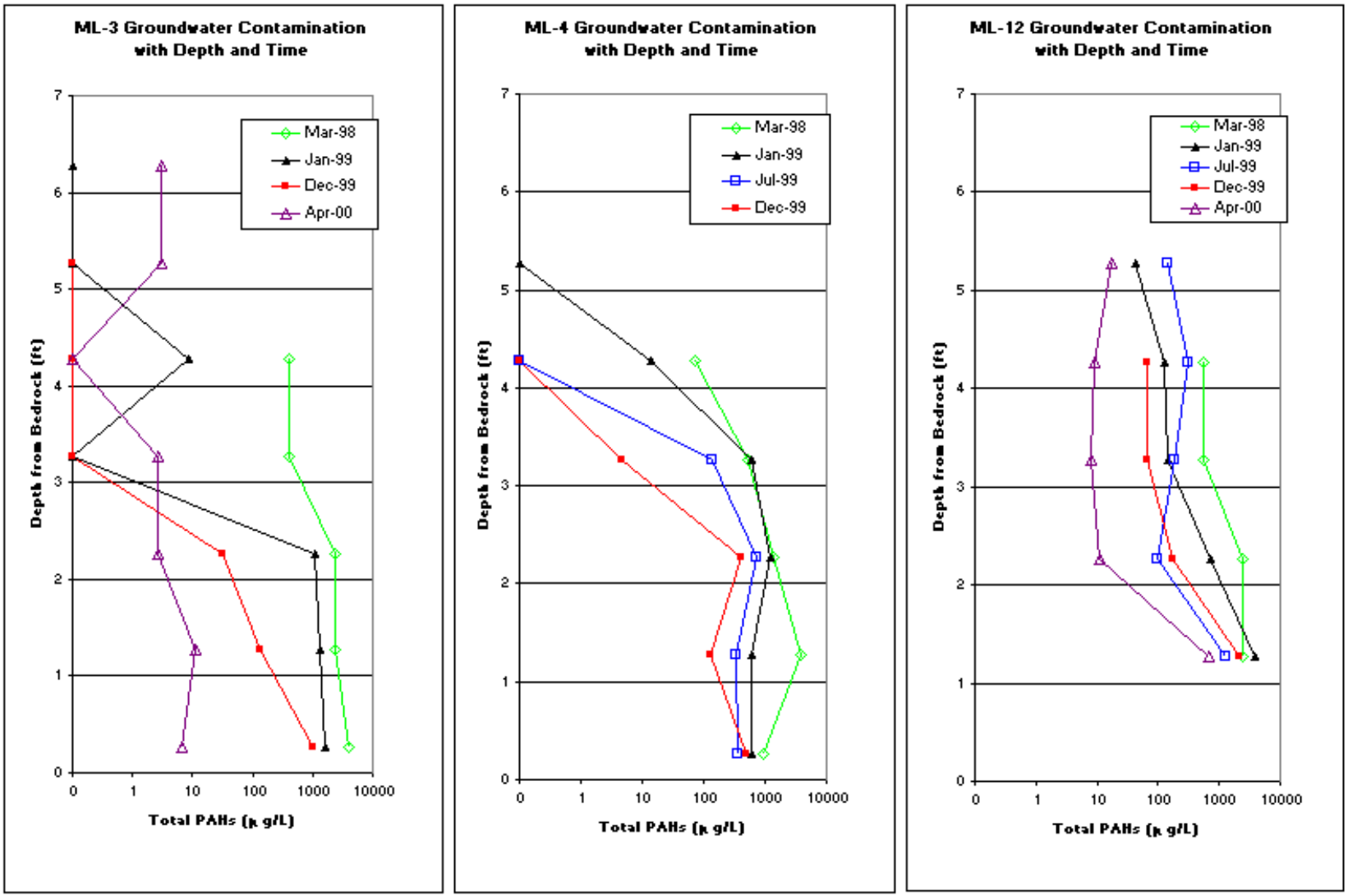

Figure 4.7: Change in Total PAH Concentration (µg/L) in log scale with Depth and Time for ML-3, 4 and 12.

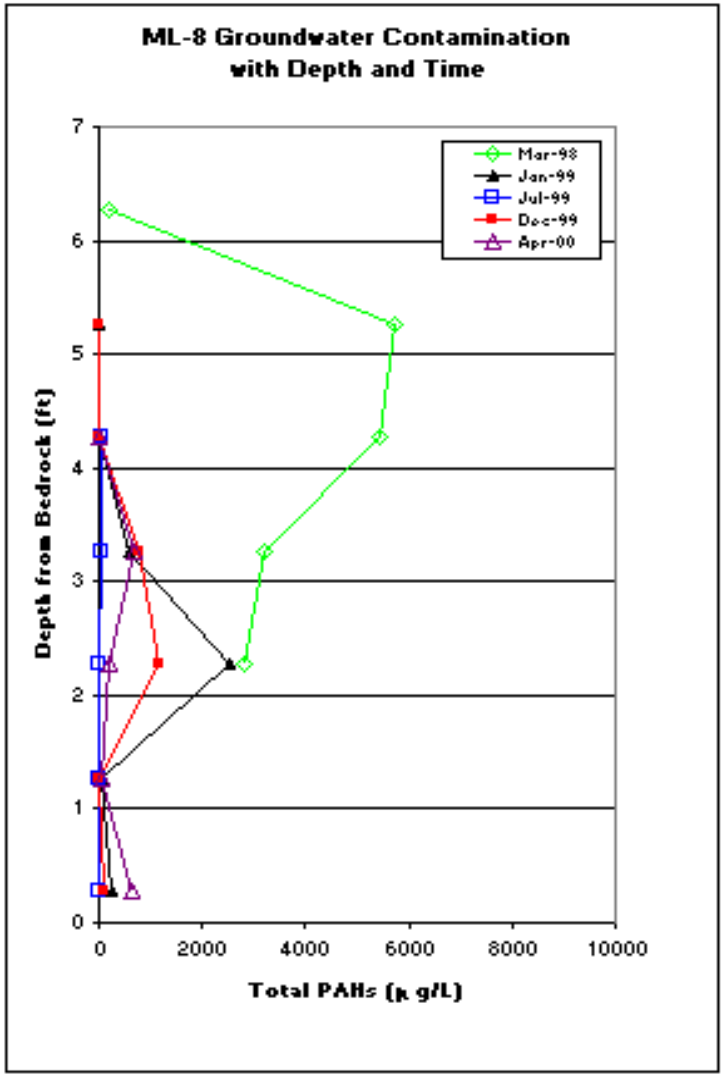

Figure 4.8: Change in PAH Concentration (mg/L) with depth and time for ML-8.

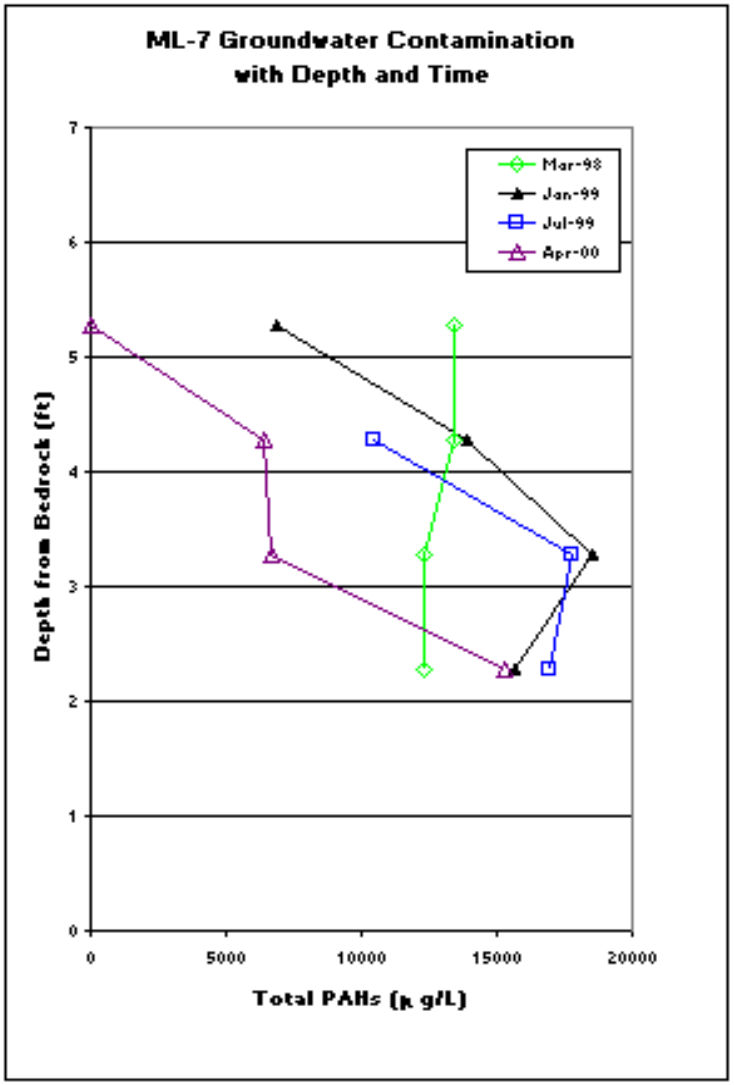

Figure 4.9: Change in PAH Concentration (mg/L) with depth and time for ML-7.

When the interceptor trench was installed and became operational in January 1998, it was designed to intercept any contamination that would have been carried by groundwater flow into Pine Creek. ML-8, 9 & 10 were installed behind the trench to monitor its effectiveness. Figure 4.8 reveals the decrease in total PAHs in ML-8 from the extremely high levels seen in March 1998 to the almost undetectable levels of July 1999. These results were quite encouraging from a regulatory standpoint as they suggest that the trench was achieving its intended purpose. However, some contamination reappeared in December 1999, indicating that there is probably still some free product or creosote sorbed to the solid phase between the trench and ML-8. PAHs that were sorbed may have solubilized into rainwater and reached ML-8. Samples taken April 2000 show a large decrease in PAH concentration from December 1999, although measurable concentrations are still present as of the last sampling. ML-9 and ML-10 have shown very little contamination since the first PAH samples were taken in March 1998.

The most contaminated area on site falls between ML-16, ML-7, and ML-11 (see Figure 4.2). From our geological profile it appears that there is a low-point in the bedrock in this area where the DNAPL tends to collect. This area seems resistant to remedial efforts, possibly because the PAH levels are high enough to inhibit root penetration and prevent an active population of microorganisms from developing. However, the growth in the contaminated areas is equivalent to that in uncontaminated areas.

Recent data, collected in April 2000, seems to indicate that some cleanup is occurring (Figure 4.9), but future investigation is needed to confirm this. However, it appears that additional remedial measures, beyond natural attenuation or indigenous biodegradation, are required to meet cleanup goals for this highly contaminated area.

Groundwater contamination data can be found in the Appendix as Tables 1A through 4A.

4.2.2 Soil Contamination

Soil contamination on-site was determined by taking soil samples from two transects (see Figure 4.1) and testing them for six prominent PAHs. Figure 4.10 illustrates the decrease in chrysene (a four-ring PAH) concentration with time over

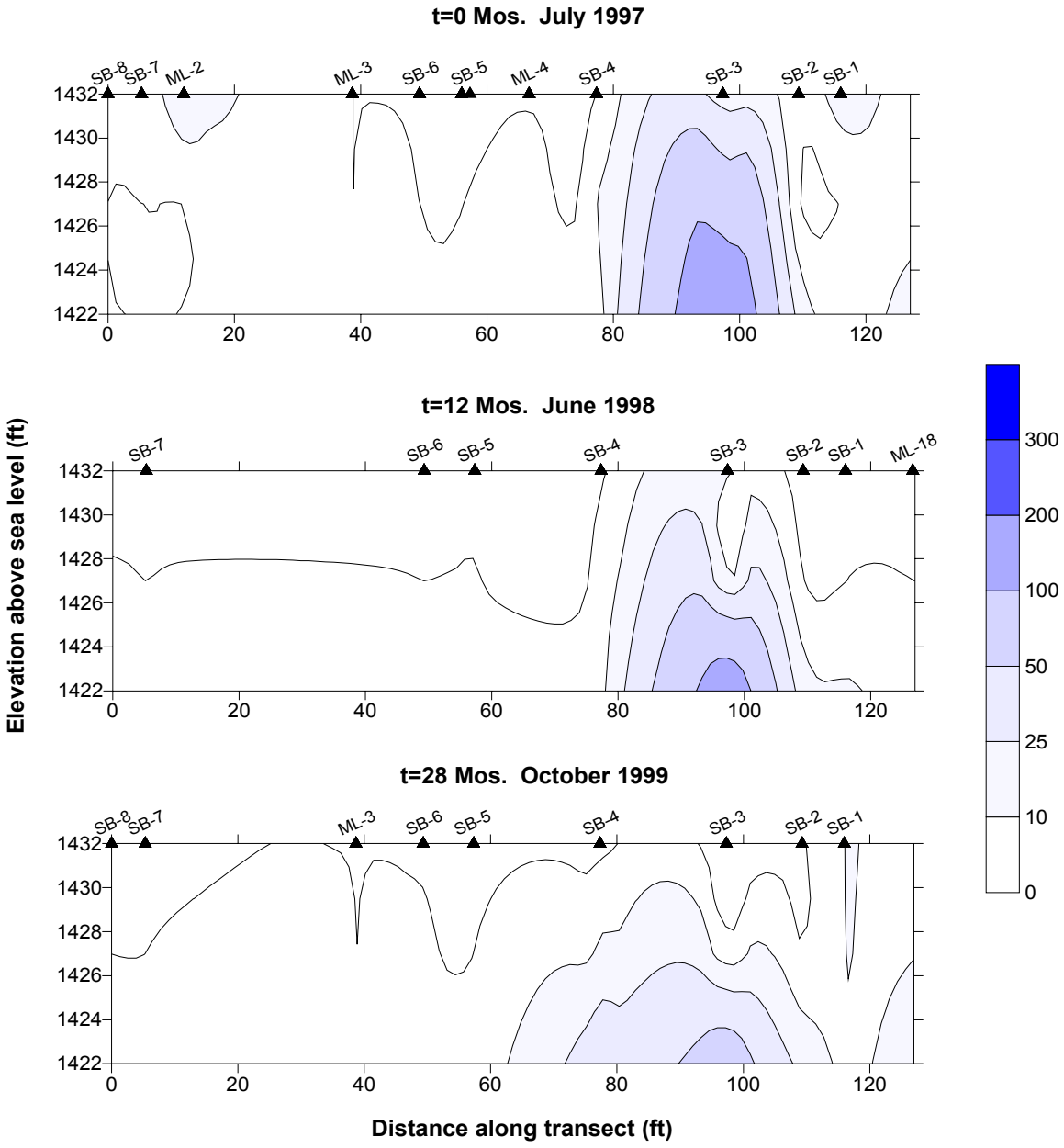

Transect One: Soil Concentration (mg/kg) Depth Profile for Chrysene

Figure 4.10: Chrysene Concentrations (mg/kg) over Time for Soil Transect 1

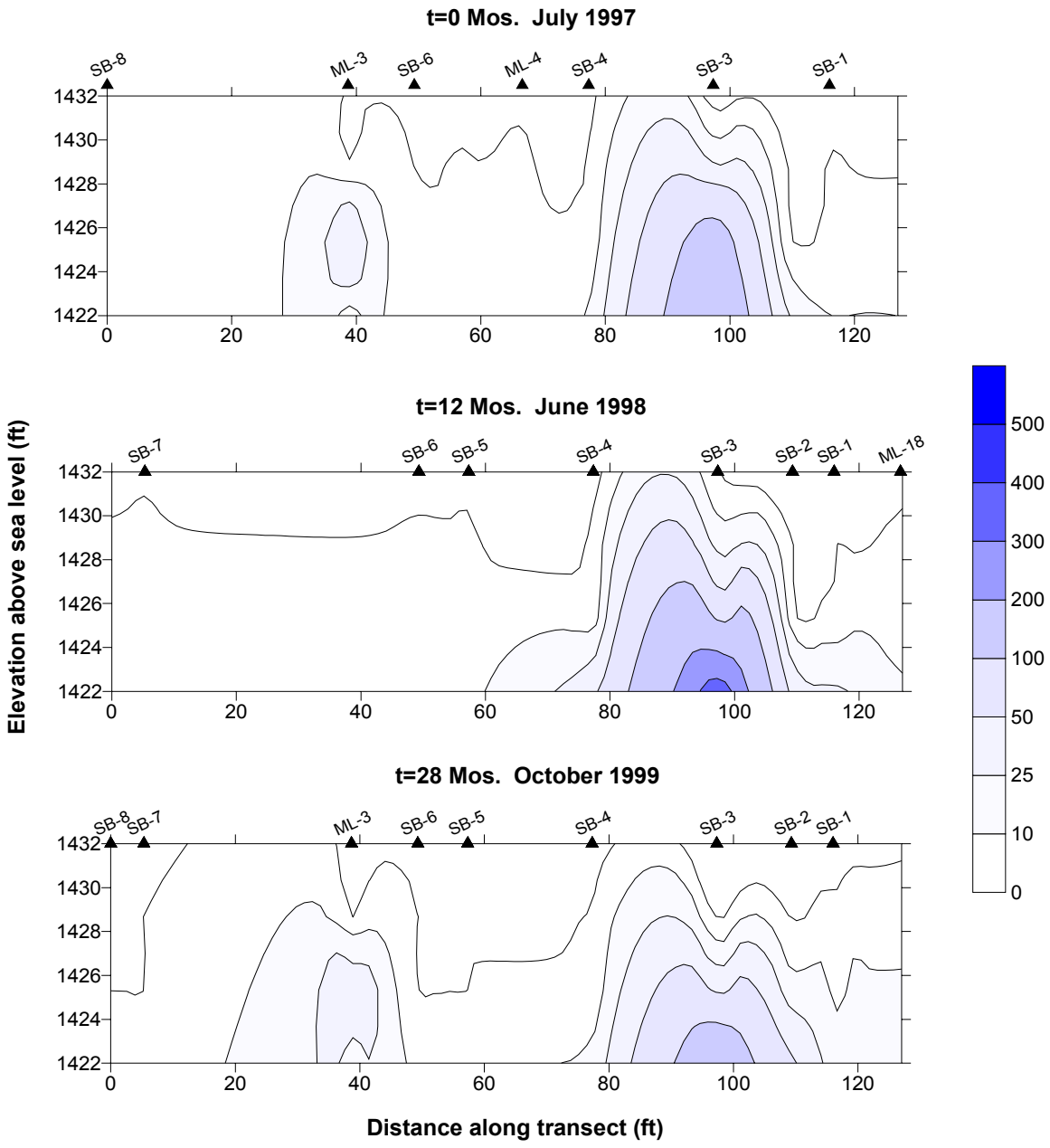

Transect One: Soil Concentration (mg/kg) Depth Profile for Fluorene

Figure 4.11: Fluorene Concentration (mg/kg) over Time for Soil Transect 1

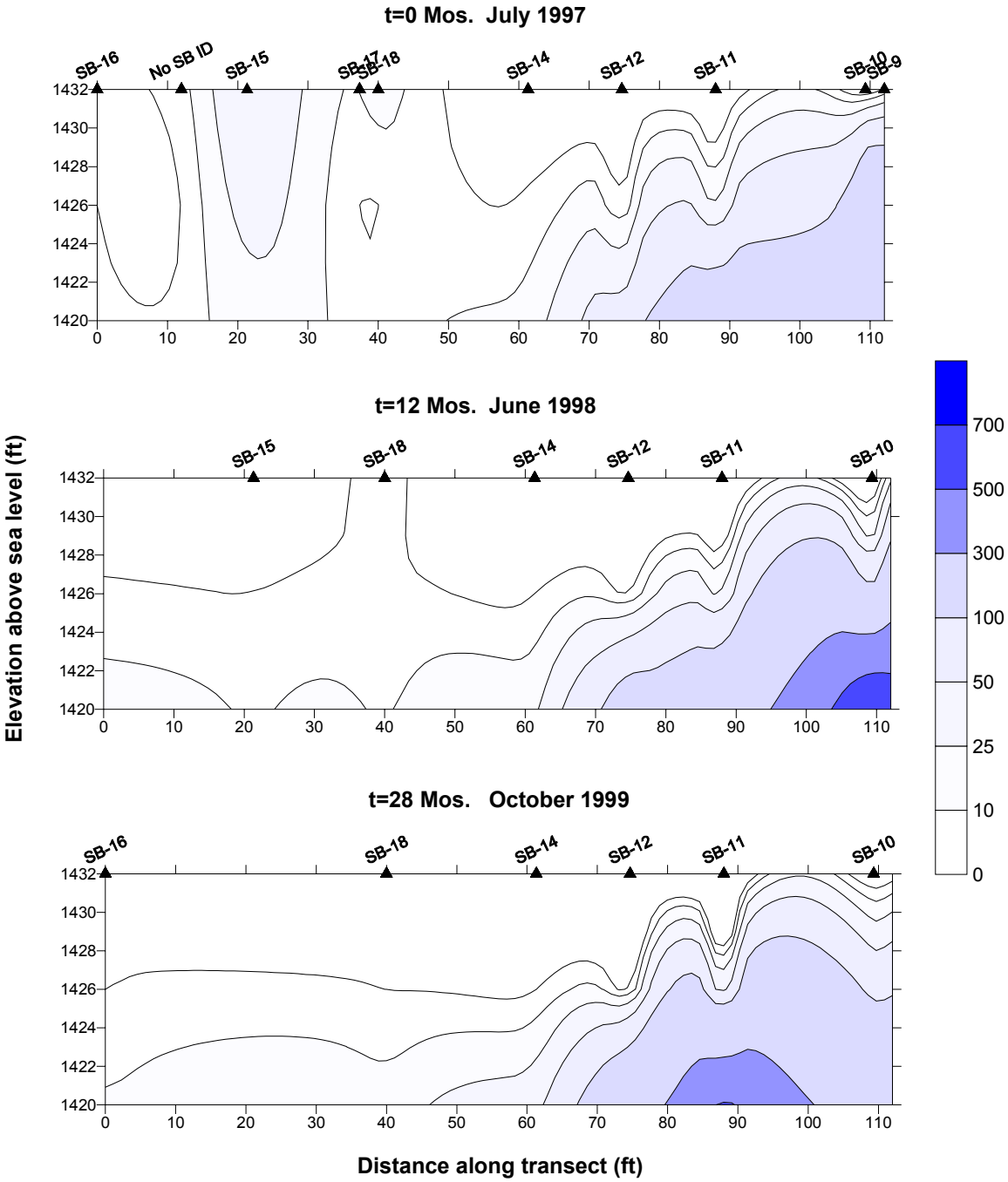

Transect Two: Soil Concentration (mg/kg) Depth Profile for Chrysene

Figure 4.12: Chrysene Concentrations (mg/kg) over Time for Soil Transect 2

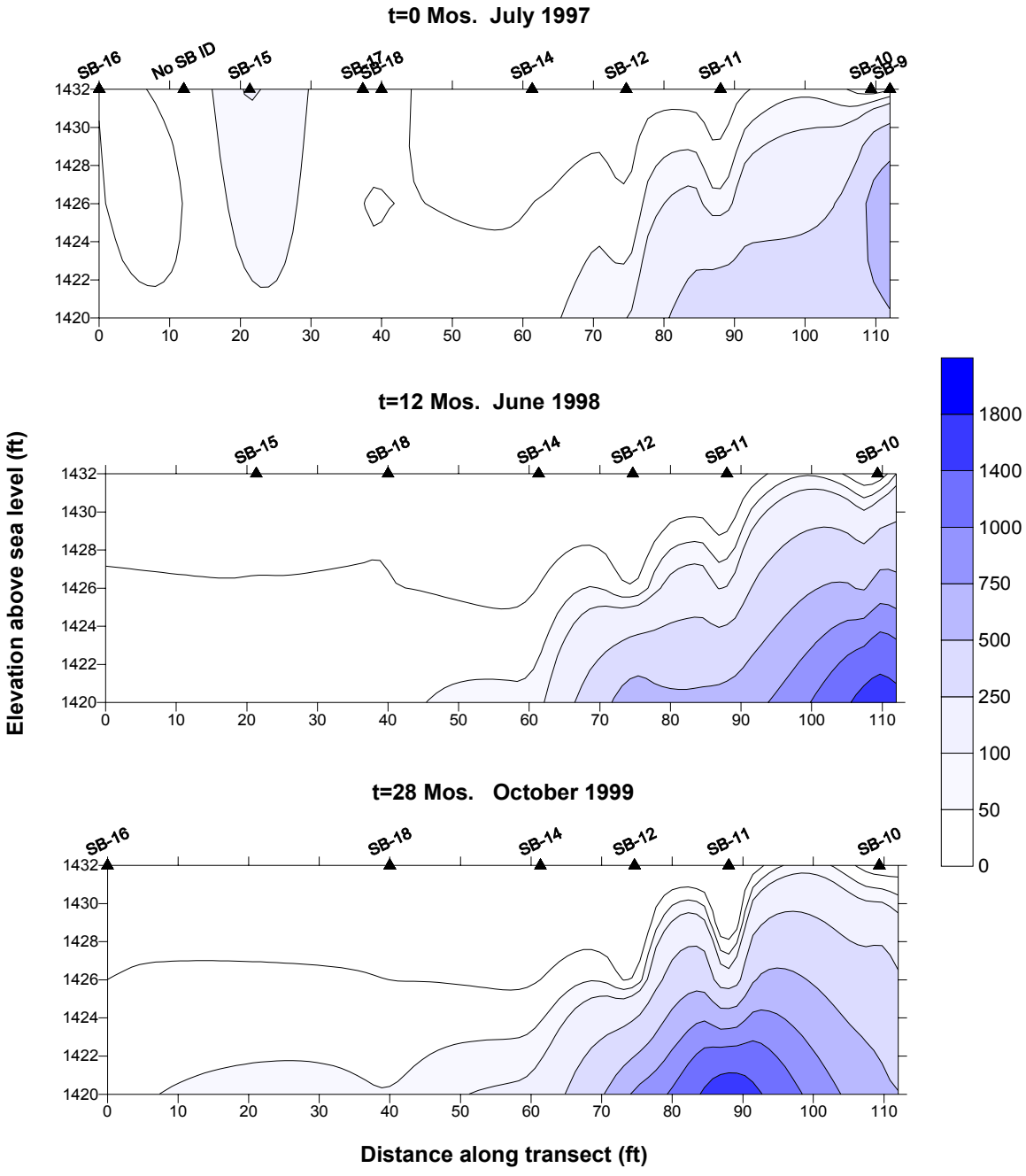

Transect Two: Soil Concentration (mg/kg) Depth Profile for Fluorene

Figure 4.13: Fluorene Concentration (mg/kg) over Time for Soil Transect 2

Transect 1. Creosote contamination just above bedrock remains high, but it appears to have undergone some remediation since samples were first tested in 1997. Figure 4.11 illustrates the changes in the concentration of fluorene (a three-ring PAH) over the same time period. PAH data for Transect 2 is showing less progress than for Transect 1 (Figures 4.12 and 4.13). Transect 2 intersects the low spot in the bedrock (Section 4.2.1), and creosote is probably collecting in that area, making it extremely difficult to remediate.

As the trees continue to grow and their roots penetrate deeper into the subsurface, and as natural attenuation processes continue, we hope to see improvement in even the most contaminated areas. Figures 4.12 and 4.13 reveal the changes over time in chrysene and fluorene concentration, respectively, for Transect 2. It appears that the DNAPL may be collecting near SB-11. Note the apparent migration of the areas of heaviest contamination from SB-10 to SB-11.

4.3 Conclusions

Based on testing of groundwater and soil parameters, site remediation has made measurable progress under natural attenuation and phytoremediation. Remediation is particularly pronounced around Transect 1 (see Figures 4.1 and 4.2), but is proceeding more slowly in the more contaminated regions near Transect 2, where high creosote contamination may be inhibiting phytoremediation and biodegradation. We have yet to determine whether natural means will be adequate to clean up the most contaminated areas of the site, especially close to bedrock.

Multi-level samplers which have consistently shown a lack of PAH contamination are defined as "Outside the Contaminant Plume." MLSs 1, 5, 9, 10, 19, 20 and 21 are categorized as such for the purposes of this study.

The complex nature of the site and the proximity of Pine Creek required the use of several remediation strategies, including phytoremediation, natural attenuation, construction of a barrier trench, and groundwater containment by both pumping and root uptake and transpiration by poplars. The focus of the next two chapters is on natural attenuation processes, specifically the investigation of *in-situ* natural biodegradation of PAHs using groundwater data. This was achieved by evaluating the status of terminal

electron acceptors in the groundwater (Chapter 5) and relating these redox parameters to the levels of PAH contamination (Chapter 6).

CHAPTER 5. REDOX CONDITIONS IN THE SITE AQUIFER

5.1 Introduction

Both aerobic and anaerobic degradation play important roles in removing organic contaminants from aquifers. Both biological and abiotic, chemical reduction of TEAs is thermodynamically possible in the subsurface. But many reactions, although thermodynamically feasible, occur too slowly, due to kinetic limitations, to have a significant impact on contaminant remediation (Schwarzenbach, et al., 1993). Microorganisms utilize enzymes that can speed these reactions by many orders of magnitude, enabling the same reactions to proceed at much faster rates.

The preference for TEAs in microbially-mediated reactions in the subsurface generally follow the sequence listed in Figure 2.1. The order in which terminal electron acceptors (TEAs) are depleted is thought to be determined by the amount of free energy (ΔG) that is generated by the oxidation of that TEA to the corresponding reduced end-products.

The primary purpose of this chapter is to attempt to discern the redox status of the subsurface environment by analyzing inorganic groundwater parameters. Focus will be on terminal electron acceptors (DO, nitrate, sulfate were monitored) and their reduced end-products (Fe(II) & sulfide were monitored). Investigation of the coal layer and its effects on subsurface chemistry will also be examined.

5.2 Oxic Conditions in the Aquifer

In remediative efforts that rely on microbial degradation of organic contaminants, aerobic conditions are usually most advantageous. When oxygen is present in the aqueous phase, thermodynamic conditions are optimal for biologically mediated degradation.

Figure 5.1 illustrates the broad range of oxygen levels in groundwater at the site. Although all the samples were less than saturated (9.2 mg/L at 20^{o} C), roughly half of the samples contained measurable oxygen. Opinions vary, but conditions are generally considered aerobic if more than about $3*10^{-4}$ atm (0.128 mg/L) dissolved oxygen is present (Snoeyink and Jenkins, 1980).

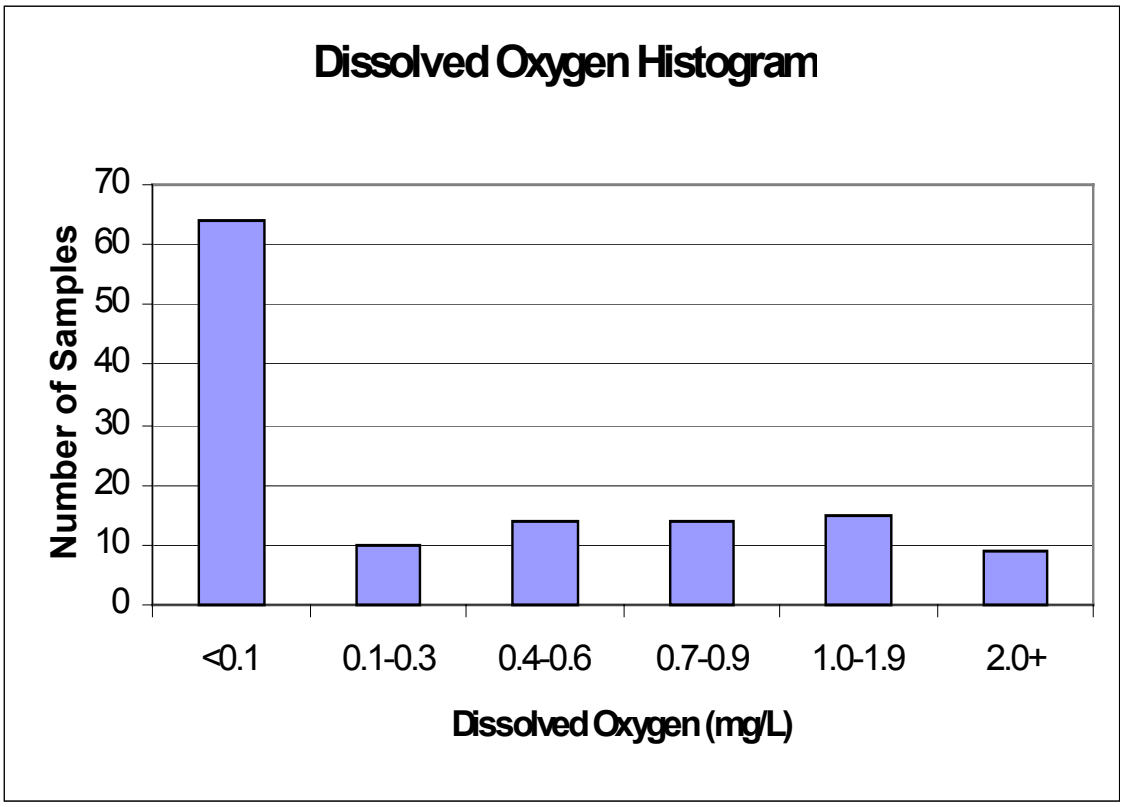

Figure 5.1: Histogram of Dissolved Oxygen Concentration (mg/L) over the Site for Samples Taken in June, July and December 1999.

The distribution of DO with depth over Transect 1 is illustrated in Figure 5.2. The shallower samples generally contain more oxygen, especially shortly after groundwater recharge. In most cases, sampling occurred shortly after rain events.

It is hypothesized that, following a recharge event, oxygen levels will drop rapidly in contaminated areas of the site as DO is quickly consumed by aerobic microorganisms. Unfortunately, extensive sampling both preceding and following a rain event is not available to confirm this hypothesis.

Many areas on our site experience aerobic conditions, but they are most prevalent at shallower depths and in areas of less contamination. See the sample data in Appendix Table 1A.

5.3 Anoxic Conditions in the Aquifer

In areas with adequate contaminant or other suitable substrates, oxygen is rapidly consumed once introduced into the subsurface and other elements will then serve as TEAs. Often a redox series develops and convention holds that the remaining TEAs are depleted sequentially.

Oftentimes there develops a spatial as well as temporal succession of redox reactions. In general, in the most contaminated region of a plume, conditions will be the most reducing (for example, sulfate reducing or methanogenic). Moving in from oxic, uncontaminated areas of the site toward the center of the plume can reveal the successive depletion of TEAs in the order illustrated in Figure 2.1.

5.3.1 Weakly Reducing Conditions

After the oxygen has been depleted, the controlling reaction in the subsurface is the biologically mediated reduction of nitrate (Figure 2.1). Figure 5.3 illustrates the relationship between nitrate and DO on-site. It includes 123 data points taken in June, July, and December 1999 for which both DO and nitrate were measured. Note the four zones as they will be used describe the relationship between the two electron acceptors.

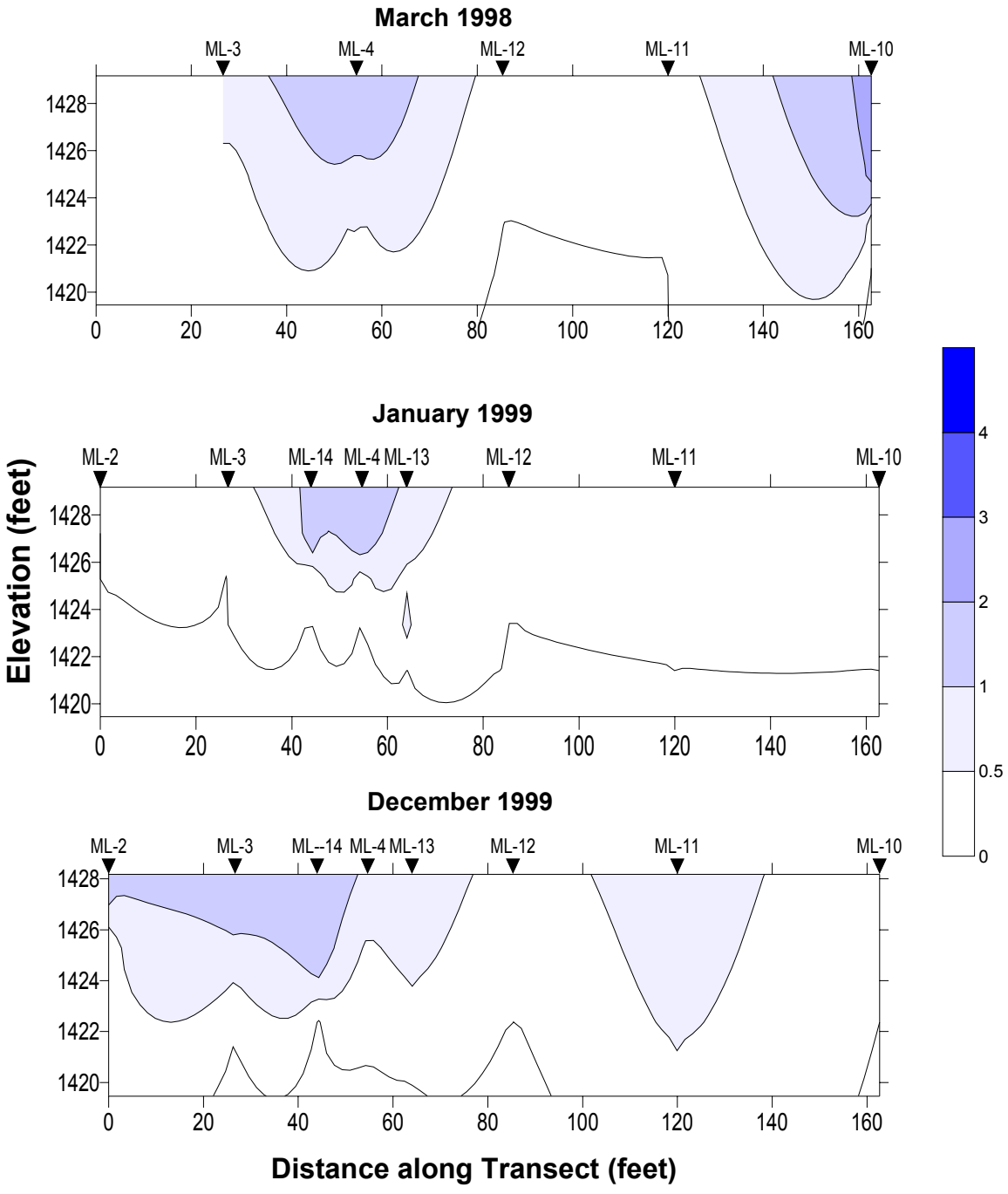

Figure 5.2: Changes in Groundwater Dissolved Oxygen Concentration (mg/L) over Time for Transect 1.

Zone 1 contains the 58 points for which both DO and nitrate were detected in measurable quantities. Where there was measurable DO, in nearly all cases we found measurable nitrate. This is to be expected, as, generally, the depletion of nitrate in groundwater should only commence once DO is consumed. There need not be a correlation between the exact quantities of DO and nitrate in a particular groundwater sample. However, the presence of both indicates that either (1) there is little bioactivity in this particular area of the subsurface and conditions are oxidized or (2) the sample was taken soon enough after recharge that the TEAs were not yet depleted.

Zone 2 contains very few points (only three), as expected. According to convention, when nitrate is zero (has been fully depleted), oxygen should have also been depleted as it would have been preferentially reduced before nitrate. The few points that do fall on the x-axis may be a result of experimental error in measuring either DO or nitrate.

Zone 3 includes those 24 points that fall on the y-axis, which contain significant nitrate but no DO. The conventional explanation would be that the oxygen has been reduced either biologically or chemically, but the nitrate either (1) has not yet been depleted because of kinetic limitations or (2) will remain in solution because prevailing redox conditions do not preclude its existence. This interpretation appears to be consistent with what we know about subsurface conditions on-site. The conditions illustrated in Zone 3 are defined herein as "weakly reducing."

Zone 4 includes only those 28 points for which both DO and nitrate measured zero or were below detection limits. When neither nitrate nor oxygen are present, it reveals that more reducing conditions exist on-site.

Average nitrate values were calculated for those samples which did, and those which did not contain oxygen (Table 5.1). Higher average nitrate values in those samples which contain DO is further evidence that nitrate concentration is closely related to redox conditions, and that nitrate is likely being used as an electron acceptor on-site. Average nitrate concentrations may be lower for points outside the coal layer because the decreased pH of areas affected by the coal layer may hinder nitrate reducing bacteria in the subsurface.

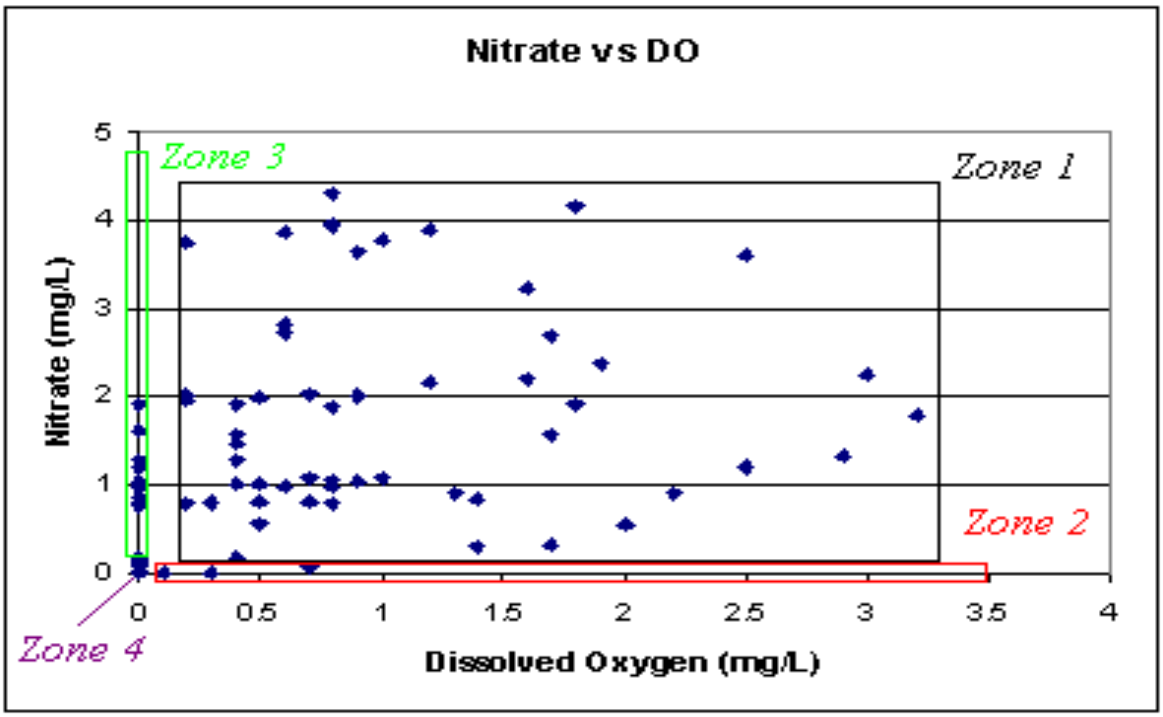

Figure 5.3: Dissolved Oxygen vs. Nitrate Concentrations for Samples Taken in June, July, and December 1999.

Table 5.1: Mean and Median Values of Nitrate and Fe(II) in the Presence and Absence of Dissolved Oxygen.

	Nitrate (mg/L)		Fe(II) (mg/L)		
	Mean	Median	Mean	Median	
DO Present	1.72	1.52	2.59	0.65	All
No DO Present	0.37	0	24	22	Samples
DO Present	1.26	0.24	2.26	0	Samples Outside the Coal Layer
No DO Present	0.90	0.00	18.36	16	

5.3.2 Moderately Reducing Conditions

Reduction of Manganese and Iron(III) oxides generally follow the reduction of nitrate. Although Mn(IV) is a potential TEA for anaerobic oxidation of organic contaminants in the subsurface, it has not been widely investigated (Lovley, 1997). Moreover, manganese species were not monitored for this project, therefore this section will focus on the reduction of Fe(III) species to Fe(II).

Fe(III) oxides are the most abundant potential electron acceptors in the subsurface (Lovley, 1994a). But they are generally very insoluble, and their insolubility is the limiting factor in the reduction of Fe(III) to Fe(II). Because of the insolubility of Fe(III) oxides and their tendency to complex under the conditions prevalent in the subsurface, aqueous Fe(III) was not monitored. Instead aqueous Fe(II) was monitored, as it is a reduced end-product of Fe(III) reduction. It should be stated, however, that Fe(II) will often precipitate out of solution in the presence of sulfides (Kennedy et al., 1999). Most of our data, though, suggests that aqueous Fe(II) is a fairly reliable measure of redox status at the Oneida site (see Section 6.4).

Figures 5.4 and 5.5 illustrate the relationship between Fe(II) and DO for samples taken between June and December 1999. The chemical effects of the coal layer cause interference in both Fe(II) and DO (Section 5.4), so only those points outside the coal layer for which both Fe(II) and DO were measured are represented here. Higher Fe(II) measurements generally indicate that more Fe(III) has been reduced. Because Fe(III) reduction should follow long after the reduction of oxygen, high DO values correspond to redox states that would not support Fe(III) reduction. Therefore, high Fe(II) measurements should correspond to lower oxygen levels, and one can observe that that is the case from Figures 5.4 and 5.5.

High DO and high aqueous Fe(II) measurements are nearly mutually exclusive, as expected. However, given the abundance of iron-based minerals in the subsurface and their ability to slowly solubilize, it is not surprising that Fe(II) and oxygen often coexist at low levels. Although points outside the coal layer were not included in these graphs, effects of the coal layer are still seen in some down-gradient samplers.

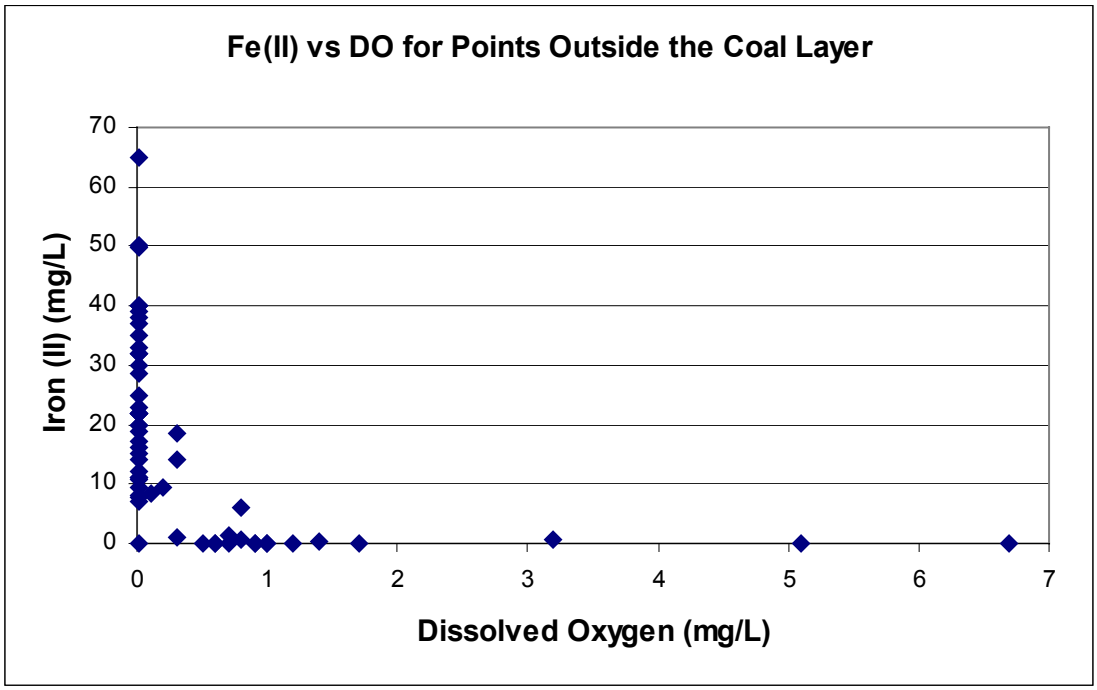

Figure 5.4: Dissolved Oxygen vs. Fe(II) Concentrations for Samples Taken in June, July and December 1999. Only those points outside the coal layer are included.

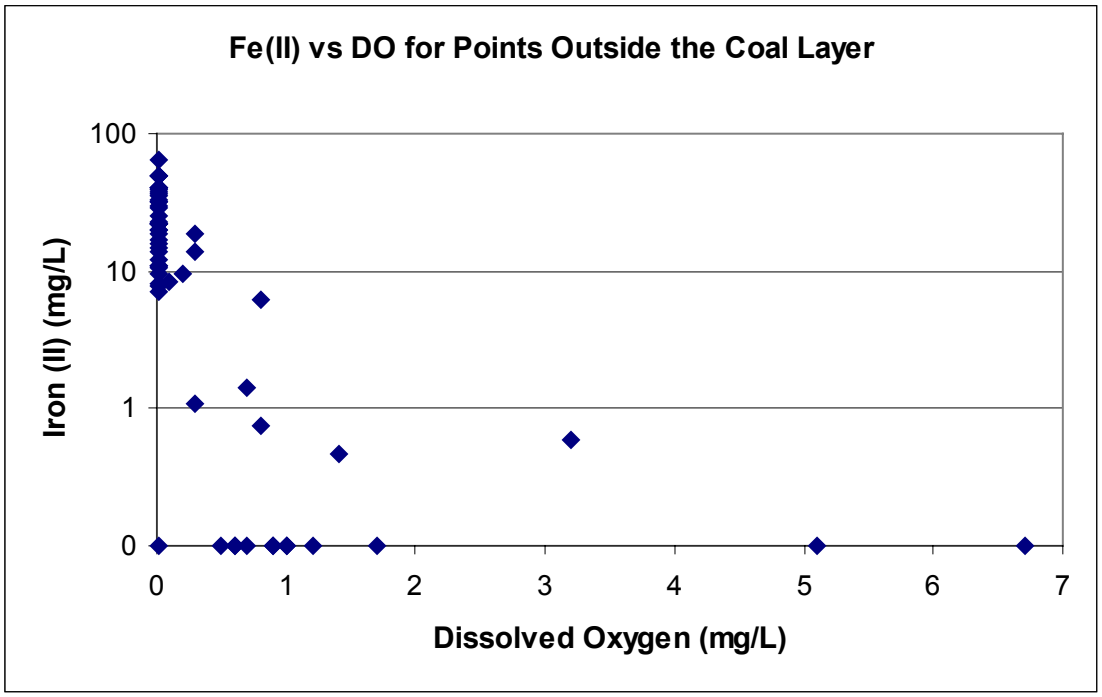

**Figure 5.5: Dissolved Oxygen vs. Fe(II) Concentrations for Samples Taken in June, July, and December 1999.
Only those points outside the coal layer are included.**

To better gauge the correlation between DO and ferrous iron, average values of Fe(II) were calculated for those samples which did, and those which did not, contain oxygen. The results are collected in Table 5.1. Because of pyrite oxidation effects due to the coal layer, averages were calculated both for the overall data and those points outside the coal layer. Higher average Fe(II) values in samples which did not contain oxygen are possibly an indication that ferrous iron concentrations are related to redox conditions and that Fe(III) may be used as a TEA in the subsurface.

5.3.3 Strongly Reducing Conditions

Sulfate reducing, fermentative, or methanogenic conditions can be defined as "strongly reducing." Despite the presence of significant sulfate on-site (see Section 5.4), there does not appear to be any strong correlation between sulfate concentration and redox status. In an effort to monitor the reduction of sulfate to sulfide, aqueous sulfide was measured in the field. However, significant sulfide concentrations were not detected between June 1999 and April 2000, the primary period of data collection in this study. It should be noted, though, that recent research indicates that aqueous sulfide may not be an adequate measure of sulfate reduction because of its tendency to precipitate out of solution when in the presence of Fe(II) (see Section 2.3.2.3).

Sulfide was detected in measurable quantities in July 2000. One possible rationale is that sulfate reducers have recently begun to thrive on-site and are just now beginning to have a major impact on the subsurface redox status. Another explanation relates to the scheduling of sampling trips. The groundwater table was often too low to obtain a thorough groundwater sampling, so we had to sample shortly after a rain event. The groundwater recharge associated with significant rain may have been enough to push the redox status of the groundwater away from the strongly reducing conditions necessary for sulfate reduction.

It is important to note that sulfate-reducers and methanogens are obligate anaerobes that are "rapidly killed by O_2 at all stages of development" (Stanier et al., 1976). Therefore, frequent recharge of oxygen-rich groundwater would probably prevent a sufficient mass of sulfate-reducing bacteria from developing and measurably reducing the elevated sulfate levels found in the aquifer.

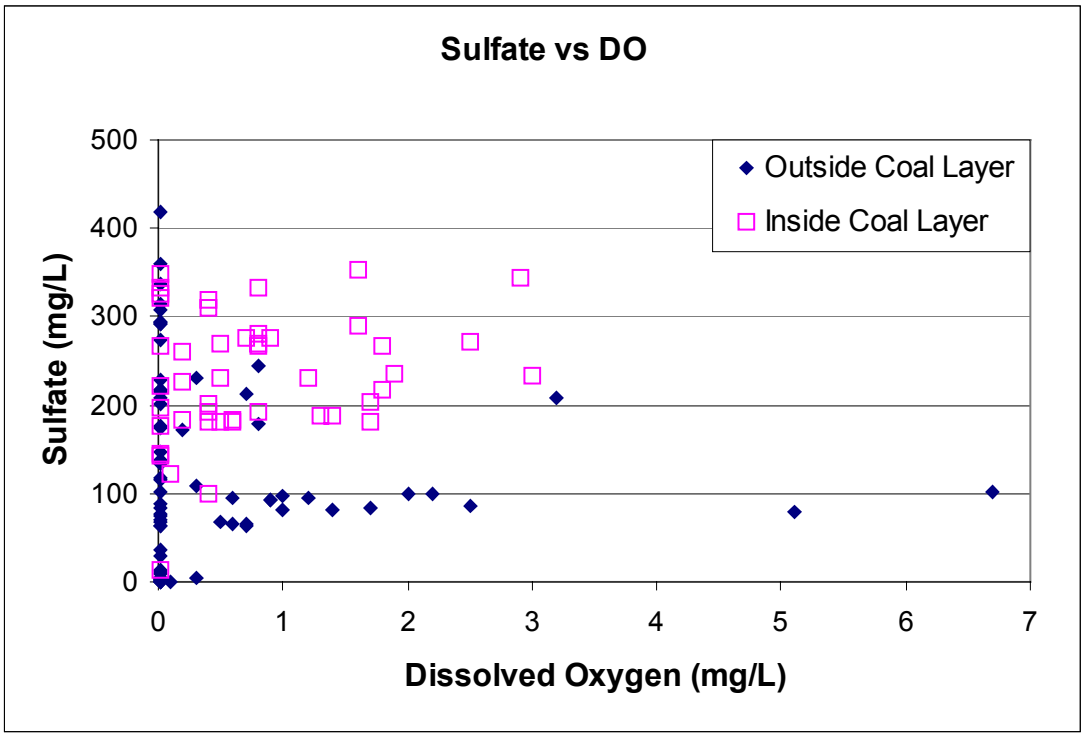

Figure 5.6: Dissolved Oxygen vs. Sulfate Concentrations for Samples Taken in June, July, and December 1999.

Table 5.2: Evidence of Pyrite Oxidation Effects from July 1999 Data for ML-20

ML Sampler	Color	pH	DO (mg/L)	Fe(II) (mg/L)	Sulfate (mg/L)	Total PAHs (mg/L)
ML20	Purple	2.95	0.0	25	333	0.0
	Red	2.52	0.0	58	348	0.0
	Yellow	2.79		59	352	0.0
	Clear	2.63		49	346	0.0

In July 2000, in addition to the more traditional geochemical analyses used throughout the project, hydrogen gas was quantified in the groundwater as a measure of subsurface redox status. Lovely et al. (1994b) state that the results of their study suggest that measuring dissolved hydrogen gas in groundwater enables one to determine the controlling terminal electron acceptor processes (TEAPs) in anoxic groundwater. The data from July indicate that sulfate-reducing and methanogenic conditions existed close to bedrock (Appendix, Table 7A). Note, though, that the July trip was unique in that it did not follow a recent rain. Such rainfall may have oxygenated even the deep sampling ports on our other sampling trips.

Figure 5.6 illustrates the lack of correlation between aqueous sulfate and DO. Instead of being correlated to redox status, it appears that sulfate concentration is more closely related to the proximity of the coal layer (Figure 5.6). This relationship will be examined in Section 5.4.

5.4 Pyrite Oxidation and the Coal Layer

The layer of discarded coal from the nearby rail yard that was not removed from the site before our investigation has introduced numerous obstacles to this project (Section 4.1). It has also given rise to chemical effects that need to be considered in order to properly assess the subsurface conditions at our site.

Some MLSs have exhibited parameters that seem to defy the typical trends on-site. For the purposes of this study, MLSs 2, 3, 4, 14 and 20 were categorized as "Inside the Coal Layer." Those closest to the coal layer (especially ML-20) were demonstrating these trends most strongly. Data from ML-20, taken in July 1999, is found in Table 5.2 and will be used to explain these trends.

Note the extremely low pH, the high sulfate and Fe(II), and the absence of both oxygen and PAHs. It appears that the areas of the site most affected by the coal layer are exhibiting pyrite oxidation, a condition similar to those found in locations affected by acid mine drainage. Below are the standard stoichiometric equations thought to describe acid mine drainage (Snoeyink and Jenkins, 1980).

$$4FeS_2(s) + 14O_2 + 4H_2O \leftrightarrow 4Fe^{2+} + 8H^+ + 8SO_4^{2-} \quad (5.1)$$

$$4Fe^{2+} + 8H^{+} + O_2 \leftrightarrow 4Fe^{3+} + 2H_2O \quad (5.2)$$

and

$$4Fe^{3+} + 12H_2O \leftrightarrow 4Fe(OH)_3(s) + 12H^{+} \quad (5.3)$$

or $$FeS_2(s) + 14Fe^{3+} + 8H_2O \leftrightarrow 15Fe^{2+} + 16H^{+} + 2SO_4^{2-} \quad (5.4)$$

Equations 5.1 and 5.2 describe the oxidation of pyrite to Fe(III). The Fe(III) can then either precipitate out of solution as ferric hydroxide or remain available to oxidize more pyrite to Fe(II). The two possible outcomes are described by equations 5.3 and 5.4. From the above equations we can see that oxygen would be consumed and hydrogen ions and sulfate would be produced. If the reaction given in the fourth equation occurred at a significant frequency in our case, Fe(II) would also be produced.

The ML-20 data in Table 5.1 represents the highest sulfate and Fe(II) levels detected at our site, as well as the lowest average pH. Also, neither oxygen nor PAHs were detected in ML-20 during the sampling period. In most cases, low DO values indicate PAH contamination (Section 6.2), but it is evident from equation 5.1 that any oxygen in the groundwater could be chemically reduced under these conditions.

5.5 Conclusions

In summary, consistent relationships can be seen between the inorganic redox-related parameters that were monitored. There are clearly zones of different redox status on-site and oxygen, nitrate, and Fe(III) are being reduced in some regions of the subsurface. Over the course of the project, data do not suggest that strongly anaerobic conditions (sulfate reducing and methanogenic) exist on-site, although recent data casts doubt on this hypothesis. Data also support the theory that pyrite oxidation effects are controlling the chemical conditions in regions of the subsurface most influenced by the coal layer.

CHAPTER 6. RELATIONSHIPS BETWEEN GROUNDWATER PAHS AND REDOX PARAMETERS

6.1 Introduction

Previous discussion (Chapter 4) documents the temporal and spatial trends in PAH contamination at our site. As shown in Chapter 5, a broad range of oxidation-reduction conditions exist in the subsurface. This chapter examines the relationship between groundwater PAH contamination and the inorganic species that serve as indicators of redox status.

6.2 Total PAHs and Dissolved Oxygen

Figures 6.1 and 6.2 illustrate the relationship between Total PAHs (TPAHs) and DO in the groundwater. It is readily evident from the figure that TPAHs and DO are nearly mutually exclusive. This supports the hypothesis that PAHs are the primary substrate in the subsurface, and that microbially mediated degradation of PAHs occurs under aerobic conditions in most areas of the site. According to Cerniglia and Heitkamp (1989), there are a variety of bacteria that can utilize PAHs as the primary carbon and energy source under aerobic conditions.

Eliminating those points most influenced by the coal layer eliminated most samples which contained neither oxygen nor PAHs. This indicates that they are largely the result of chemical effects produced by the coal layer. Section 5.4 details cases in which oxygen depletion near the coal layer is linked to chemical reactions associated with the occurrence of pyrite oxidation.

6.3 Total PAHs and Nitrate

It is widely believed that nitrate is the next preferred electron acceptor following oxygen depletion (Figure 2.1). As Figures 6.3 and 6.4 illustrate, the relationship between TPAHs and nitrate shows the same general trend as that between TPAHs and DO. Namely, samples with nitrate greater than roughly 1.0 mg/L had little or no PAH contamination while those with high PAHs generally had low or undetectable nitrate concentrations. Note the concentration of points on the y-axis in Figure 6.4.

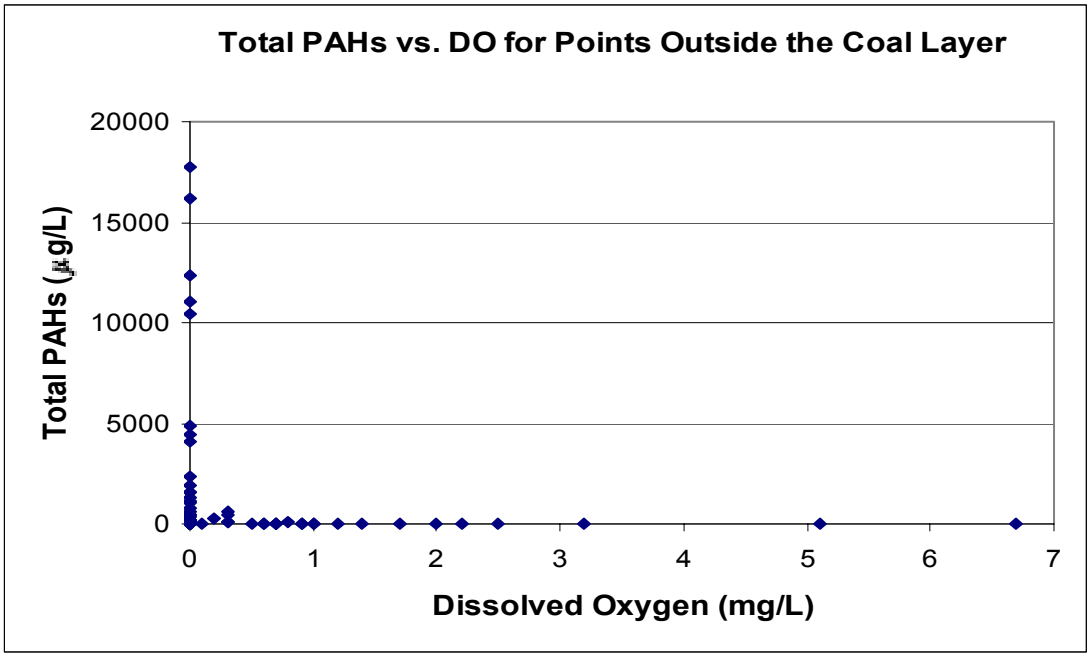

**Figure 6.1: Total PAHs vs. Dissolved Oxygen Concentrations for Samples Taken in June, July and December 1999.
Only those points outside the coal layer are included.**

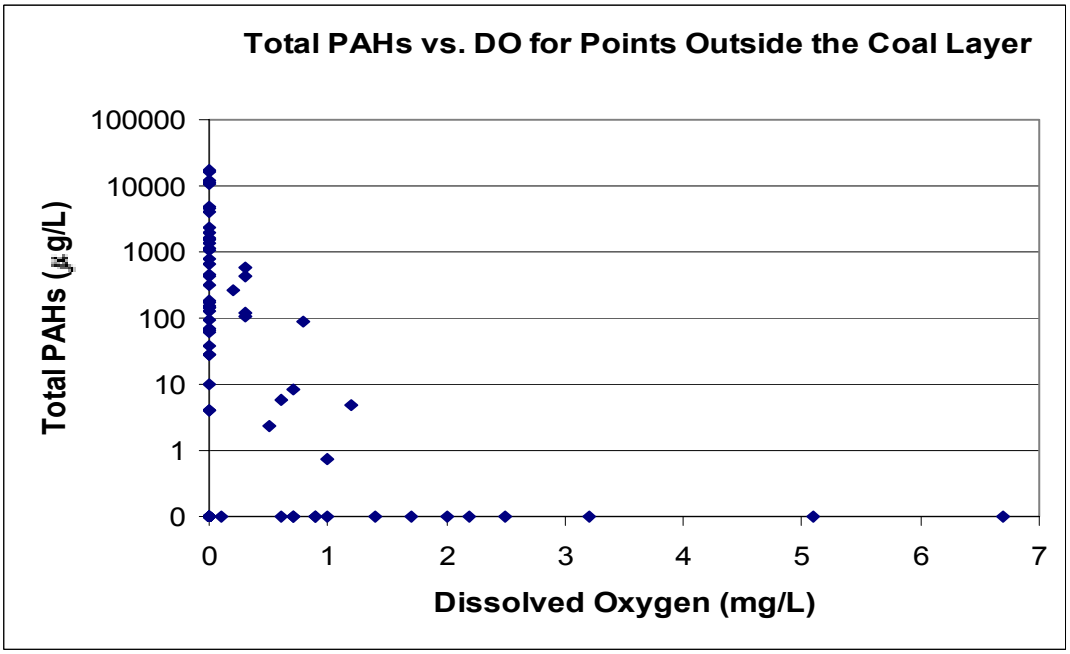

**Figure 6.2: Total PAHs vs. Dissolved Oxygen Concentrations for Samples Taken in June, July and December 1999.
Only those points outside the coal layer are included.**

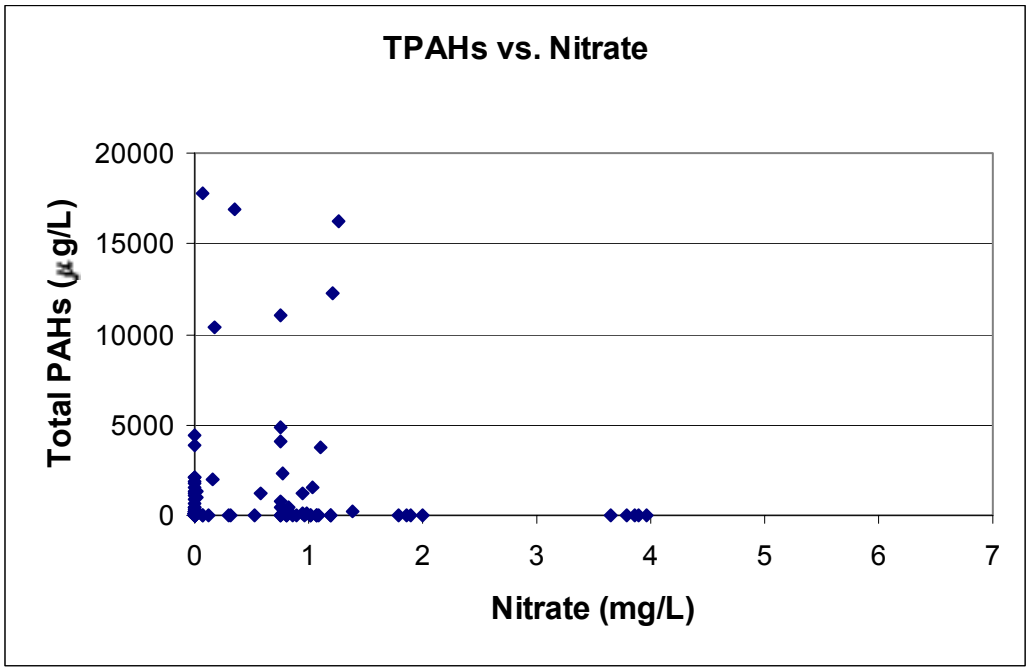

Figure 6.3: Total PAHs vs. Nitrate Concentrations for Samples Taken in June, July and December 1999.
Only those points outside the coal layer are included.

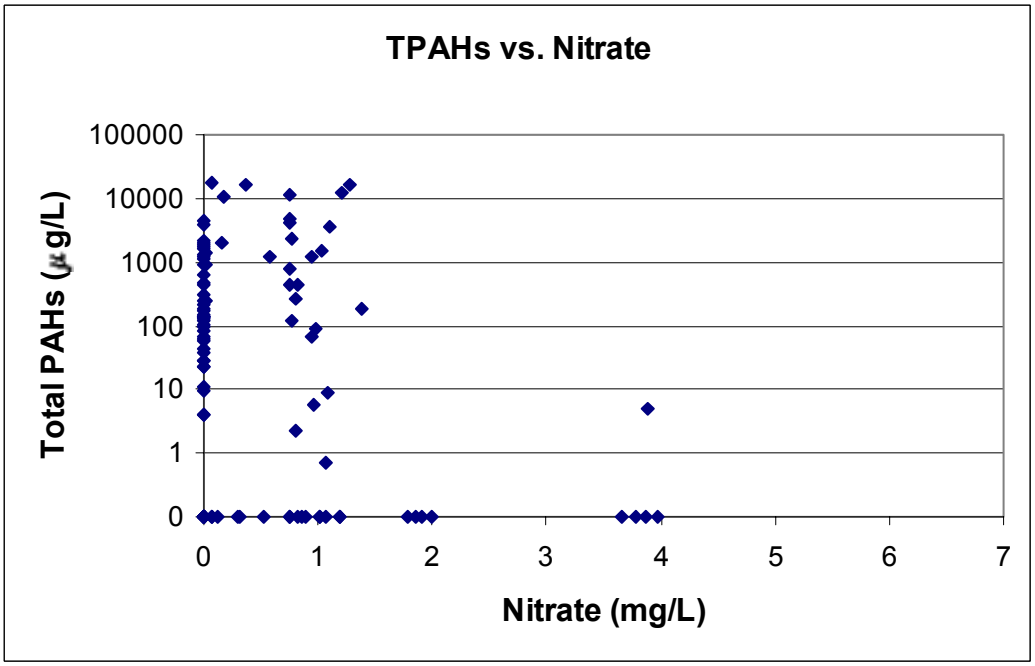

Figure 6.4: Total PAHs vs. Nitrate Concentrations for Samples Taken in June, July and December 1999.
Only those points outside the coal layer are included.

Samples with significant PAHs and measurable nitrate suggest non-equilibrium conditions and, thus, one possible explanation for the variation from the expected trend is kinetics. Sampling trips were usually planned around groundwater recharge events to ensure that the groundwater table was high enough to collect a sufficient number of samples. Oxygen-rich rainwater supplies a shallow aquifer with an abundant source of the preferred TEA, making denitrification less advantageous to subsurface microbes. If sampling was conducted shortly after rainfall it is likely that the nitrate in a sample would not yet be depleted by the time the sample was tested.

The presence of nitrate in the most contaminated samples may indicate that such high concentrations of PAHs may be toxic to denitrifiers and nitrate reducers. The lack of precision in nitrate analysis procedures conducted at the lab is another feasible reason for the coexistence of nitrate and PAHs. Nitrate levels may have been overestimated in some samples that contained very little nitrate because of inconsistent standard curves.

6.4 Total PAHs and Iron Species

Figure 6.5 illustrates the relationship between Fe(II) and TPAHs at our site. The many samples with appreciable Fe(II) reflect that anoxic conditions prevail in much of the aquifer since, in the presence of O_2 or nitrate, Fe(II) should be oxidized to Fe(III). There is no obvious correlation between TPAH and Fe(II) and many samples without any PAHs contain significant Fe(II). However, all of the samples with high TPAHs (2000 ppb or more) contain at least 10 mg/L of Fe(II). Also note that the samples with very little Fe(II) (<3 mg/L) contain almost no PAHs.

An explanation for the presence of high Fe(II) in those samples without PAHs can be found in the discussion of the coal layer and its chemical effects in Section 5.4. Of particular importance is Equation 5.4.

Samples outside the contaminant plume were removed from Figure 6.6 to better gauge the impact of the presence of PAHs on Fe(II) concentration. There is a definite upward trend in these points, providing further evidence of the possibility of degradation of PAHs by Fe(III) reducing bacteria.

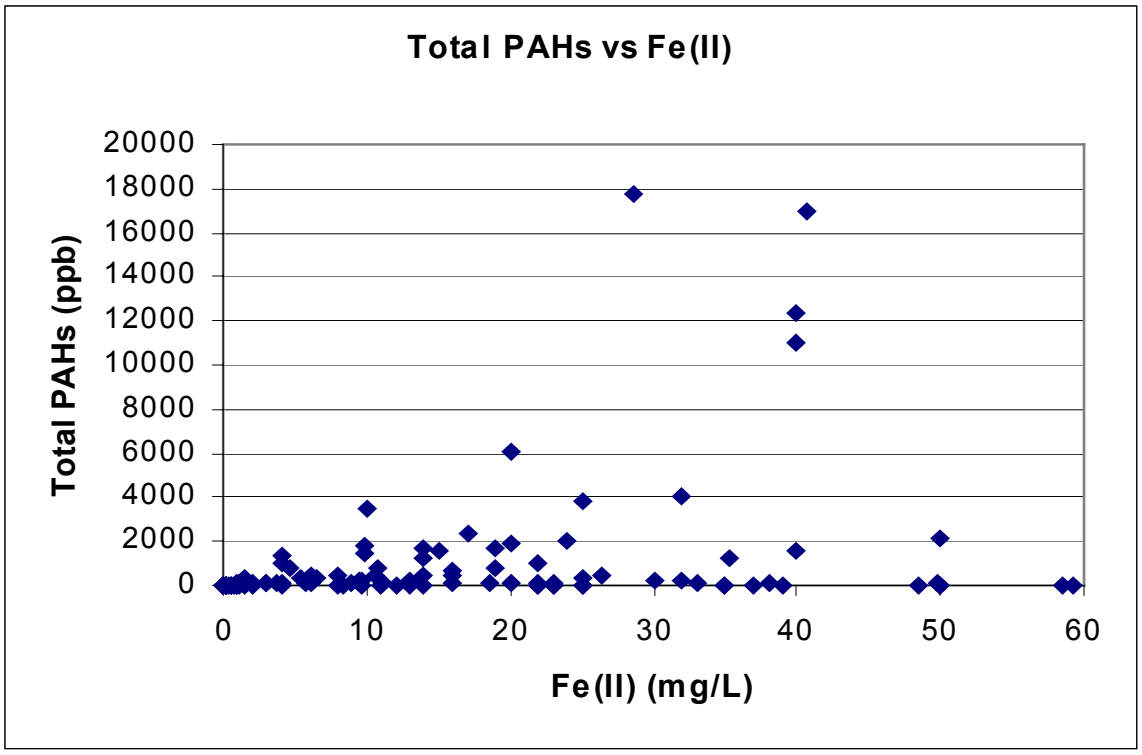

Figure 6.5: Total PAHs vs. Fe(II) Concentrations for Samples Taken in June, July and December 1999.

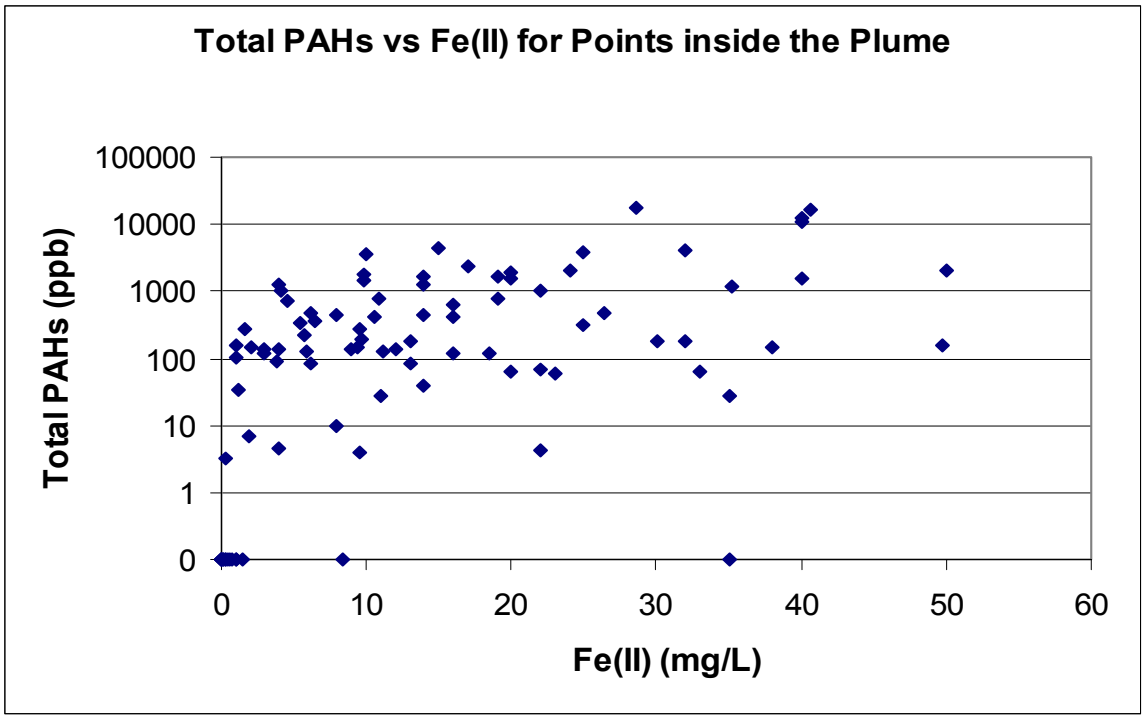

Figure 6.6: Total PAHs vs. Fe(II) Concentrations for Samples Taken in June, July and December 1999. Only points inside the contaminant plume are included.

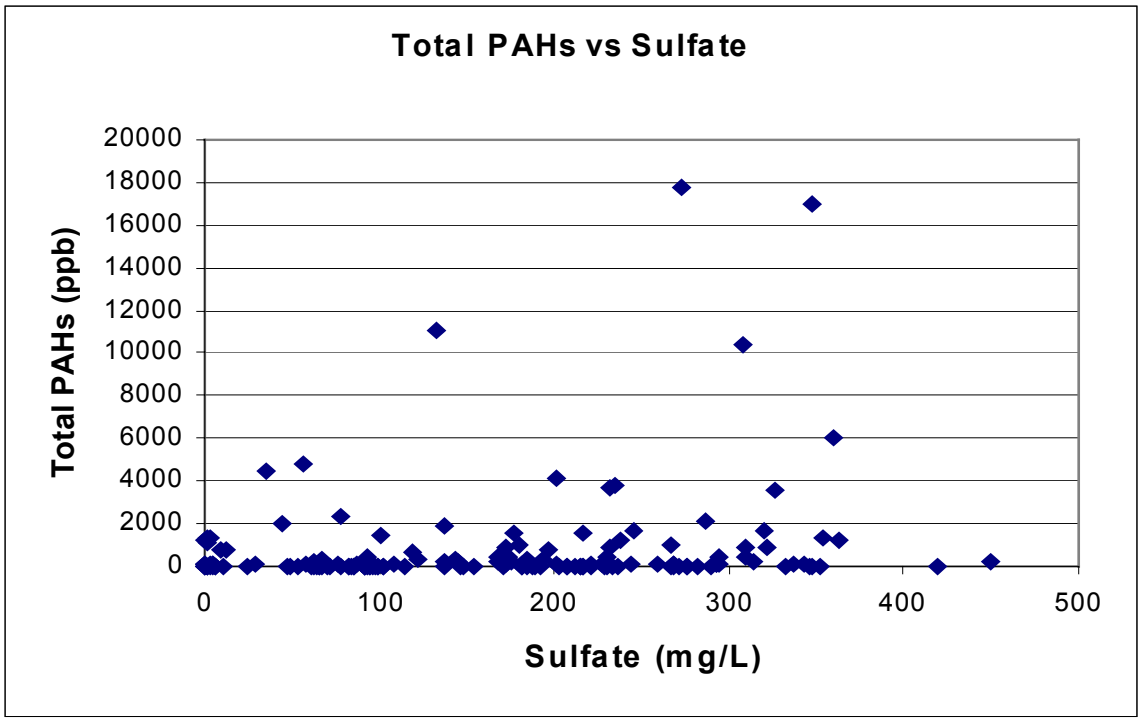

Figure 6.7: Total PAHs vs. Sulfate Concentrations for Samples Taken in June, July and December 1999.

6.5 Evidence of Sulfate Reducing and Methanogenic Conditions

Highly anaerobic aquifers are characterized by loss of sulfate as an electron acceptor and the accumulation of dissolved end-products like sulfide, and in the case of extremely anaerobic conditions, methane. Because of potential interference in sulfide analyses (Section 2.3.2.3), its use as an indicator of sulfate reduction was limited. It should be noted, however, that significant sulfide was not found in any samples taken between June 1999 and April 2000, the primary period of data collection for this study.

Figure 6.4 presents TPAH levels as a function of the corresponding sulfate concentrations. From this figure, it is clear that substantial sulfate levels were measured in both uncontaminated samples and those with extreme PAH contamination. This data suggests that PAH degradation may not readily occur in the field using sulfate as an electron acceptor. Several possible explanations can be offered.

Kinetic limitations and the abundance of sulfate present in the coal layer may create the impression that sulfate is not being reduced when it actually is. The coal layer supplies copious amounts of sulfate to the aquifer and, unless degradation rates were extremely high, sulfate would not be fully depleted by sulfate-reducers. It is also possible that indigenous sulfate-reducers may not be able to use PAHs as their sole carbon and energy source in the field. However, Coates et al. (1996) showed that it is possible with pure cultures in a lab study.

Another possible explanation is that the system was buffered by the large amount of Mn(IV) or Fe(III) oxides present (Stumm and Morgan, 1996). If there was an excess supply of Fe(III) or Mn(IV) in bioavailable, aqueous form, then the less thermodynamically-advantageous reduction of sulfate would probably not occur frequently. Pyrite oxidation could provide an abundant source of aqueous Fe(III) (Section 5.4). Finally, sulfate-reducers are obligate anaerobes, so the recharge of oxygen-rich groundwater could preclude their existence on-site, especially close to the ground surface (Stanier et al., 1996).

Given the recent July 2000 data, however, and its implication that sulfate-reducing and methanogenic conditions do exist in the subsurface (Section 5.3.3), the most likely explanation is that a number of effects conspired to lead us to the conclusion that sulfate was not being used as a TEA. First, the July 2000 sampling was scheduled when

there had been no recent rainfall, whereas previous sampling was done shortly after recharge events. In addition, sulfate is plentiful in the aquifer and aqueous sulfide is not a reliable measure of sulfate reduction in the subsurface.

The reality is probably that sulfate is used as a TEA in the degradation of PAHs in the aquifer, but groundwater recharge created oxidized conditions and sulfate-reduction ceased while we were sampling. After a period during which oxygen did not reach deeper regions of the aquifer, sulfate-reducers and methanogens could possibly recover and begin to thrive. If true, sulfate would provide a plentiful supply of TEAs at our site, perhaps making natural biodegradation a better long-term remediation solution than previously believed.

6.6 Conclusions

There is ample evidence to conclude that the bioremediation of creosote compounds in the subsurface is occurring on-site. Relationships between PAHs and redox parameters demonstrate that high TPAH counts are consistently associated with more reducing conditions.

Depletion of oxygen and nitrate are both correlated to the presence of PAHs. Also, the presence or absence of Fe(II) seems to be linked to TPAH levels, although positive interference caused by the chemical effects of the coal layer make this harder to determine. Evidence of sulfate reduction will have to be investigated further before a determination can be made on the relationship between sulfate-reduction and PAH contamination.

CHAPTER 7. CONCLUSIONS

The following are the major findings of this study:

- Remediation has progressed considerably since monitoring began in 1997. The contaminant plume has decreased in size and many of the individual multi-level samplers have shown consistently decreasing levels of contamination.
- Based on analyses of TEAs and their reduced endproducts, a wide range of redox conditions exist in the site aquifer. It appears that oxygen, nitrate, and Fe(III) are being reduced in different regions of the subsurface.
- Bioremediation of creosote compounds is taking place in the aquifer. Relationships between PAHs and redox parameters demonstrate that high TPAH levels are consistently associated with more reducing conditions.
- Depletion of oxygen and nitrate can both be correlated to the presence of PAHs. Also, the presence or absence of Fe(II) seems to be linked to TPAH levels, although positive interference caused by the chemical effects of the coal layer make this harder to determine.
- The coal layer produces pyrite oxidation chemical effects, resulting in conditions similar to those encountered in acid mine drainage.
- Recent data indicates that the possibility of active sulfate-reduction and methanogenesis on-site cannot be discounted. If sufficient numbers of sulfate-reducing bacteria are present in the subsurface, excess sulfate from the coal layer would supply an almost unlimited source of electron acceptors. Further investigation of the role of PAH utilization under sulfate-reducing and methanogenic conditions is warranted for a more complete understanding of the role of microbially-mediated degradation in the overall remediation of the site.

LITERATURE CITED

American Water Works Association (AWWA). 1995 *Standard Methods for the Characterization of Water and Wastewater*. 19th Edition, Denver, CO.

Cerniglia, C.E. and M.A. Heitkamp. 1989 Microbial Degradation of Polycyclic Aromatic Hydrocarbons (PAH) in the Aquatic Environment. In: *Metabolism of Polycyclic Aromatic Hydrocarbons in the Aquatic Environment.* CRC Press, Inc., Boca Raton, pp. 41-68.

Coates, J.D., J. Woodward, J. Allen, P. Phillip, and D.R. Lovley. 1997 Anaerobic Degradation of Polycyclic Aromatic Hydrocarbons and Alkanes in Petroleum-Contaminated Marine Harbor Sediments. *Appl. Environ. Microbiol.* Vol. 63, 3589-3593.

Coates, J.D., R.T. Anderson, and D.R. Lovley. 1996 Oxidation of Polycyclic Aromatic Hydrocarbons under Sulfate-reducing Conditions. *Appl. Environ. Microbiol.* Vol. 62, 1099-1101.

Cornelissen, G., H. Rigterink, M.M.A. Ferdinandy, and P.C.M. van Noort. 1998 Rapidly Desorbing Fractions of PAHs in Contaminated Sediments as a Predictor of the Extent of Bioremediation. *Environ. Sci. Technol.* Vol. 32, 966-970.

Fetter, C.W. 1993 *Contaminant Hydrology.*, Second Edition. Prentice Hall, Upper Saddle River, NJ.

Fetterolf, G. 1998 Characterization of a Creosote-contaminated Tie Yard Site and the Effects of Phytoremediation. Masters Thesis, Virginia Polytechnic Institute and State University.

Geraghty and Miller, Inc. 1997. Supplemental Site Investigation Report: Norfolk Southern Corporation Oneida Tie Yard Site. Oak Ridge, TN.

Kennedy, L.G., J.W. Everett, T. Dewers, W. Pickins, and D. Edwards. 1999 Application of Mineral Iron and Sulfide Analysis to Evaluate Natural Attenuation at Fuel Contaminated Site. *J.of Env. Eng.* Vol. 125, 47-56.

Leduc, R., R. Samson, B. Al-Bashir, J. Al-Hawari, and T. Cseh. 1992 Biotic and Abiotic Disappearance of Four PAH Compounds from Flooded Soil under Various Redox Conditions. *Wat. Sci. Tech.* Vol. 26, 51-60.

Lovley, D.R., J.C. Woodward, and F.H. Chapelle. 1994a Stimulated Anoxic Biodegradation of Aromatic Hydrocarbons Using Fe(III) Ligands. *Nature* Vol. 370, 128-131.

Lovley, D.R., F.H. Chapelle, and J.C. Woodward. 1994b Use of Dissoved H_2 Concentrations to Determine Distribution of Microbially Catalyzed Redox Reactions in Anoxic Groundwater. *Environ. Sci. Technol.* Vol. 28, 1205-1210.

Lovley, D.R., J.D. Coates, J.C. Woodward, and E.J. Phillips. 1995 Benzene Oxidation Coupled to Sulfate Reduction. *Appl. Environ. Microbiol*. Vol. 61, 953-958.

Lovley, D.R.. 1997 Potential for Anaerobic Bioremediation of BTEX in Petroleum-contaminated Aquifers. *J. Ind. Micro. Biotech.* Vol. 18, 75-81.

Malachova, K. 1999 Using Short-term Mutagenicity Tests for the Evaluation of Geotoxicity of Contaminated Soils. *J. Soil Contam.* Vol. 8, 667-680.
Matso, K. 1995 Mother Nature's Pump and Treat. *Civil Engineering*. Vol. 65, 46-49.

Mihehcic, J.R., and Luthy, R.G. 1988a Degradation of Polycyclic Aromatic Hydrocarbon Compounds under Various Redox Conditions in Soil-Water Systems. *Appl. Environ. Microbiol.* Vol. 54, 1182-1187.

Mihehcic, J.R., and Luthy, R.G. 1988b Microbial Degradation of Acenaphthene and Naphthalene under Denitrification Conditions in Soil-Water Systems. *Appl. Environ. Microbiol.* Vol. 54, 1188-1198.

Mueller, J.G., P. Chapman and P. Pritchard. 1989 Creosote-contaminated Sites. *Environ. Sci. Technol.* Vol. 23, 1197-1201.
Prentice-Hall, Inc. Englewood Cliffs, NJ.

Rockne, K.J., and S. Strand. 1998 Biodegradation of Bicyclic and Polycyclic Aromatic Hydrocarbons in Anaerobic Enrichments. *Environ. Sci. Technol.* Vol. 32, 3962-3967.

Rockne, K.J., J.C. Chee-Sanford, R.A. Sanford, B. Hedlund, J.T. Staley, and S.E. Strand. 1999 Naphthalene Degradation and Mineralization by Nitrate-Reducing and Denitrifying Pure Cultures. In: *Bioremediation Technologies for Polycyclic Aromatic Hydrocarbon Compounds*, Battelle Press, pp. 191-196.

Rutherford, M.P, M.R. Gray, and M.J. Dudas. 1997 Desorption of [^{14}C]Naphthalene from Bioremediated and Nonbioremediated Soils Contaminated with Creosote Compounds. *Environ. Sci. Technol.* Vol. 31, 2515-2519.

Sawyer, C.N., P.L. McCarty, and G.F. Parkin. 1994 *Chemistry for Environmental Engineering*., Fourth Edition, McGraw-Hill, Inc., New York.

Snoeyink, V.L. and D. Jenkins. 1980 *Water Chemistry*, John Wiley & Sons, Inc. New York.

Stanier, R.Y., E.A. Adelberg, and J.L. Ingraham. 1976 *The Microbial World,* Prentice-Hall, Inc. Englewood Cliffs, NJ..

Stumm, W. and J.J. Morgan. 1996 *Aquatic Chemistry*, Third Edition, Wiley-Interscience, New York.

Sved, D.W., M. Roberts, Jr., and P. Veld. 1997 Toxicity of Sediments Contaminated with Fractions of Creosote. *Wat. Res.* Vol. 31, 294-300.

Tang, J., M.J. Carroquino, B.K. Robertson, and M. Alexander. 1998 Combined Effect of Sequestration and Bioremediation in Reducing the Bioavailability of Polycyclic Aromatic Hydrocarbons in Soil. *Environ. Sci. Technol.* Vol. 32, 3586-3590.

Trepte, Bjorn. 1999 Fe(III) Ligands as Oxidants to Enhance Bioremediation. In: *Bioremediation Technologies for Polycyclic Aromatic Hydrocarbon Compounds*, Battelle Press, pp. 229-233.

Zhang, W., E. Bouwer, and W. Ball. 1998 Bioavailability of Hydrophobic Organic Contaminants: Effects and Implications of Sorption-Related Mass Transfer on Bioremediation. *Ground Water Monitoring & Remediation*. Vol. 18, 126-138.

APPENDIX

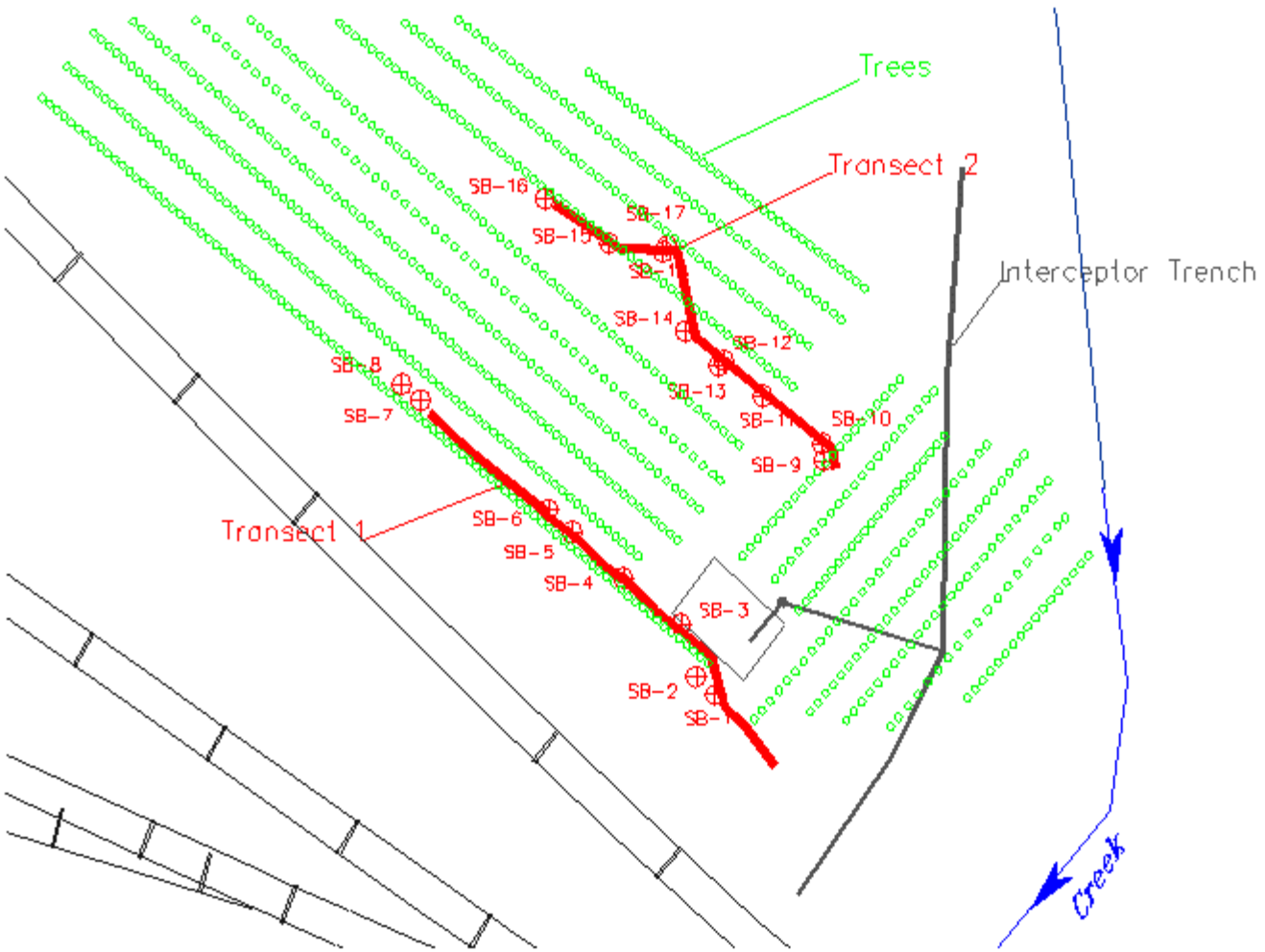

Figure 1A: Site Map with Soil Boring and Transects Labeled

Table 1A: July 1999 Groundwater Data

MLS	Sampler	Depth above Bedrock (ft)	TPAHs (ppb)	pH	DO (mg/L)	NO_3^- (mg/L)	Fe(II) (mg/L)	SO_4^{2-} (mg/L)
ML-2	Blue	6.27	0.0	5.51			0.2	
	Green	5.27	3.3	5.29	3.0	2.3	0.3	233
	Orange	4.27	0.0	4.40	1.9	2.4		236
	Purple	3.27	6.9	5.46	1.2	2.2	2.0	230
	Red	2.27	148.0	3.76	0.2	2.0	9.4	227
	Yellow	1.27	977.8	5.16	0.5	1.0		181
	Clear	0.27				0.1		147
ML-3	Green	5.27	0.0	4.09	2.5	3.6	0.0	271
	Orange	4.27	0.0	3.93	0.8	4.0	0.0	268
	Purple	3.27	0.0	3.92	1.8	4.2	0.0	267
	Red	2.27	158.5	3.86	0.80	4.3	1.0	268
	Yellow	1.27	120.2	3.79	0.20	3.8	3.0	259
	Clear	0.27				3.7		262
ML-4	Orange	4.27	0.0	3.74	0.80	3.9	0.0	192
	Purple	3.27	135.6	3.58	0.40	1.9	4.0	201
	Red	2.27	747.1	3.84	0.00	0.0	4.6	197
	Yellow	1.27	328.3	4.71	0.10	0.00	5.5	122
	Clear	0.27	363.1	4.49	0.00	0.00	6.5	144
ML-6	Red	2.27	1720.5	5.15		0.00	19.0	246
ML-7	Orange	4.27	10418.2	4.33	0.00	0.18		309
	Purple	3.27	17761.6	5.10	0.00	0.07	28.6	273
	Red	2.27	16939.6	4.00		0.36	40.7	348
ML-8	Orange	4.27	28.2	6.24	0.00	0.00	35.0	0
	Purple	3.27	62.8	6.30	0.0	0.00	20.0	0
	Red	2.27	4.1	6.46	0.0	0.00	22.0	0
	Yellow	1.27	4.1	6.55	0.0	0.00	9.6	1
	Clear	0.27	9.9	6.63	0.0	0.00	8.0	4
ML-9	Yellow	1.27	22.1	6.23		0.00		149
ML-10	Orange	4.27	0.0	6.05		0.00		137
	Red	2.27	10.8	6.23		0.00		47
	Yellow	1.27	0.0	6.42	0.0	0.00		10

ML-11	Orange	4.27	130.5	4.08	0.0	0.00	11.1	336
	Purple	3.27	428.2	4.21	0.0	0.00	10.6	294
	Red	2.27	1756.8	4.31			9.8	
	Yellow	1.27	47437.4					
ML-12	Green	5.27	142.2	5.66	0.0	0.00	38.0	76
	Orange	4.27	309.8	5.81	0.0	0.00	25.0	68
	Purple	3.27	183.1	5.90	0.0	0.00	30.0	62
	Red	2.27	95.7	5.96	0.0	0.00		29
	Yellow	1.27	1247.1	6.07		0.00	14.0	0
ML-13	Orange	4.27	639.9	5.17	0.0	0.00	16.0	118
	Purple	3.27	1910.2	5.09		0.00	20.0	136
	Red	2.27	58.5	5.71		0.00	23.0	3
	Clear	0.27	119.7	5.76		0.00	16.0	0
ML-14	Orange	4.27	0.0	5.15	1.4	0.84	0.1	188
	Purple	3.27	0.0	5.13	1.3	0.91	0.1	188
	Yellow	1.27	89.9	5.18		0.00	3.8	172
ML-16	Red	2.27	1190.7	5.04		0.58	35.3	363
	Yellow	1.27	3835.0	6.01		0.00	25.0	234
	Clear	0.27	2059.8	6.00		0.00	24.0	44
ML-17	Yellow	1.27	153.1	3.03	0.00	0.00	49.7	292
	Clear	0.27	468.3	3.50		0.00	26.5	309
ML-18	Purple	3.27	0.0	6.05	0.70	0.07	1.4	212
	Red	2.27	103.2	6.24	0.30	0.00	1.1	108
	Yellow	1.27	217.6	6.30		0.00	5.8	91
ML-20	Purple	3.27	0.0	2.95	0.00	0.00	25.0	333
	Red	2.27	0.0	2.52	0.00	0.00	58.5	348
	Yellow	1.27	0.0	2.79		0.00	59.3	352
	Clear	0.27	0.0	2.63		0.00	48.6	346
ML-21	Purple	3.27	0.0	5.53	1.70	0.32	0.0	83
	Red	2.27	0.0	5.71	1.4	0.29	0.5	82
	Clear	0.27	0.0	5.77		0.00		85

Table 2A: April 2000 Groundwater Data

MLS	Sampler	Depth above Bedrock (ft)	TPAHs (ppb)	pH	DO (mg/L)	NO_3^- (mg/L)	Fe(II) (mg/L)	SO_4^{2-} (mg/L)
ML-1	Black	7.27	3.2	5.66	0.3	0.0	1.2	199
	Blue	6.27	0.0	5.55	0.7	1.0	0.1	184
	Green	5.27	3.1	5.76	0.3	1.6	0.0	183
	Orange	4.27	2.9	5.78	0.3	1.6	0.0	181
	Purple	3.27	7.6	5.79	0.3	2.0	0.1	179
	Red	2.27	8.2	5.74	0.3	1.7	0.1	179
	Yellow	1.27	9.6	5.80	0.4	2.4	0.1	178
	Clear	0.27	10.8	6.03	0.5	1.5	0.0	182
ML-3	Black	7.27	3.0	3.78		0.5	1.7	454
	Blue	6.27	3.0	4.11	0.4	0.3	0.4	408
	Green	5.27	0.0	4.06	0.20	0.9	0.8	358
	Orange	4.27	2.7	4.29	0.20	0.9	0.5	354
	Purple	3.27	2.6	4.31	0.10	0.8	0.4	356
	Red	2.27	11.4	4.31	0.20	0.7	1.2	360
	Yellow	1.27	6.4	4.28	0.10	0.8	1.2	360
	Clear	0.27	53.7	4.31	0.10	0.5	1.2	361
ML-4	Green	5.27	0.0		0.30			
	Orange	4.27		3.97	0.10	2.36	1.1	413
	Purple	3.27		4.22	0.10		1.7	
	Red	2.27	617.9	4.12	0.10	1.91	6.2	409
	Yellow	1.27	320.7	5.07	0.00	0.00	10.3	244
	Clear	0.27	360.4	5.16	0.00	0.00	4.5	229
ML-5	Blue	6.27	0.0					
	Green	5.27	0.0			0.79		334
	Orange	4.27	0.0	5.76	0.0	0.00	36.0	301
	Purple	3.27	0.0	5.60	0.0	0.00	22.0	308
	Red	2.27	0.0	5.89	0.0	0.00	29.0	314
	Yellow	1.27	0.0					
	Clear	0.27	0.0	4.51	0.0	2.12		328

ML-7	Green	5.27	2.9	6.02			3.8	
	Orange	4.27	6378.2	5.00			9.6	
	Purple	3.27	6707.1	5.00		1.40	10.0	419
	Red	2.27	15265.0			2.25		455
	Clear	0.27				0.00		79
ML-8	Green	5.27			0.0			
	Orange	4.27	0.0	6.13			6.0	
	Purple	3.27	656.7	6.43	0.0	0.00	8.8	3
	Red	2.27	170.8	6.45	0.0	0.06	8.5	103
	Yellow	1.27	28.2	6.52	0.0	0.00	10.6	32
	Clear	0.27	634.1	6.66	0.0	0.00	7.8	13
ML-9	Red	2.27	0.0			0.00		209
	Yellow	1.27	0.0	6.27		0.00	7.6	217
ML-10	Orange	4.27	0.0	6.09	0.0	0.00	13.6	252
	Purple	3.27	13.9	6.31	0.0	0.00	9.7	209
	Red	2.27	24.5	6.32	0.0	0.00	16.7	258
	Yellow	1.27	0.0	6.37		0.00	14.9	1
ML-11	Orange	4.27	125.9	4.39	0.3	0.00	2.9	423
	Purple	3.27	207.7	4.57	0.0	0.00	2.3	421
	Red	2.27	677.0	4.78	0.0	0.00	2.1	405
	Clear	0.27	17689.0					
ML-12	Green	5.27	17.0	6.14	0.40	0.00	0.2	396
	Orange	4.27	8.9	6.19	0.10	0.00	0.1	404
	Purple	3.27	8.0	6.20	0.20	0.00	0.8	432
	Red	2.27	10.6	6.24	0.00	0.00	1.2	426
	Yellow	1.27	659.0			0.00		290
ML-13	Blue	6.27		3.48	0.30	1.99	0.9	426
	Green	5.27	0.0	3.47	0.00	1.00	2.1	460
	Orange	4.27	5.9	3.67	0.00	0.02	7.7	442
	Purple	3.27	7.9	3.82	0.00	0.00	6.9	432
	Red	2.27	0.0	3.99	0.00	0.00	10.6	443
	Yellow	1.27	217.6			0.00		65

ML-14	Blue	6.27	0.0		1.00			
	Green	5.27	0.0	5.16	0.30	1.11	0.2	399
	Orange	4.27	0.0	5.15	0.20	0.88	0.1	358
	Purple	3.27	0.0	5.25	0.20	1.10	0.1	370
	Yellow	1.27	17.6	5.12	0.20	0.00	0.4	353
ML-16	Purple	3.27	0.0					
	Red	2.27	1506.6	4.98		0.00	23.0	472
	Yellow	1.27	4295.5	5.93			31.0	
	Clear	0.27	2554.1					
ML-18	Purple	3.27	0.0	6.30	0.4	0.00	0.2	210
	Red	2.27	108.0	6.40	0.1	0.00	1.4	197
	Yellow	1.27	557.0	6.36	0.0		5.0	
	Clear	0.27	1337.4					
ML-19	Purple	3.27		6.28		0.62		166
	Red	2.27	0.0	6.03	0.8	0.45	0.2	166
	Yellow	1.27	0.0	6.29		0.00	0.1	163
	Clear	0.27	0.0					
ML-22	Orange	4.27				0.00		373
	Purple	3.27	149.7	4.35		0.00	3.0	484
	Red	2.27	429.4					
ML-23	Purple	3.27				1.67		460
	Red	2.27	319.2			0.00		521
	Yellow	1.27	318.0					
ML-24	Orange	4.27				0.00		520
	Purple	3.27	0.0					
ML-25	Orange	4.27				0.00		422
	Purple	3.27	0.0		0.0		44.0	

Table 3A: July 1999 Groundwater Data

MLS	Depth above Bedrock (ft)	Sampler	Napthalene ppb	Acenapthylene ppb	Acenapthene ppb	Fluorene ppb	Phenanthrene ppb	Anthracene ppb	Fluoranthene ppb	Pyrene ppb	Chrysene ppb
ML-2	6.27	Blue	0.0	0.0	0.0	0.0	0.0	0.0	0.0	0.0	0.0
	5.27	Green	0.0	0.0	0.0	3.3	0.0	0.0	0.0	0.0	0.0
	4.27	Orange	0.0	0.0	0.0	0.0	0.0	0.0	0.0	0.0	0.0
	3.27	Purple	0.0	0.0	2.1	4.8	0.0	0.0	0.0	0.0	0.0
	2.27	Red	101.0	0.0	20.9	13.9	12.1	0.0	0.0	0.0	0.0
	1.27	Yellow	854.6	10.5	58.6	35.3	18.8	0.0	0.0	0.0	0.0
ML-3	5.27	Green	0.0	0.0	0.0	0.0	0.0	0.0	0.0	0.0	0.0
	4.27	Orange	0.0	0.0	0.0	0.0	0.0	0.0	0.0	0.0	0.0
	3.27	Purple	0.0	0.0	0.0	0.0	0.0	0.0	0.0	0.0	0.0
	2.27	Red	109.4	5.0	22.7	11.6	9.9	0.0	0.0	0.0	0.0
	1.27	Yellow	13.1	8.5	44.7	27.2	21.2	0.0	5.4	0.0	0.0
ML-4	4.27	Orange	0.0	0.0	0.0	0.0	0.0	0.0	0.0	0.0	0.0
	3.27	Purple	0.0	5.9	73.4	26.4	8.9	0.0	11.3	9.6	0.0
	2.27	Red	109.4	19.8	256.9	139.7	182.5	14.8	0.0	24.0	0.0
	1.27	Yellow	0.0	8.5	117.7	75.5	65.5	11.8	22.5	17.1	9.6
	0.27	Clear	0.0	18.0	125.6	84.6	107.3	11.3	0.0	16.4	0.0
ML-6	2.27	Red	369.0	44.7	668.8	270.4	275.4	27.7	37.3	27.2	0.0
ML-7	4.27	Orange	9479.9	73.9	349.6	198.4	183.7	0.0	40.6	82.1	10.0
	3.27	Purple	16000.1	117.0	529.9	397.9	457.5	0.0	138.2	102.4	18.5
	2.27	Red	15267.2	121.7	573.5	334.8	504.3	0.0	81.4	56.6	0.0
ML-8	4.27	Orange	0.0	0.0	18.4	9.8	0.0	0.0	0.0	0.0	0.0
	3.27	Purple	0.0	5.7	39.3	17.8	0.0	0.0	0.0	0.0	0.0
	2.27	Red	0.0	0.0	4.1	0.0	0.0	0.0	0.0	0.0	0.0
	1.27	Yellow	0.0	0.0	4.1	0.0	0.0	0.0	0.0	0.0	0.0
	0.27	Clear	0.0	4.5	5.4	0.0	0.0	0.0	0.0	0.0	0.0
ML-9	1.27	Yellow	0.0	0.0	22.1	0.0	0.0	0.0	0.0	0.0	0.0
ML-10	4.27	Orange	0.0	0.0	0.0	0.0	0.0	0.0	0.0	0.0	0.0
	2.27	Red	0.0	0.0	10.8	0.0	0.0	0.0	0.0	0.0	0.0
	1.27	Yellow	0.0	0.0	0.0	0.0	0.0	0.0	0.0	0.0	0.0
ML-11	4.27	Orange	34.9	0.0	34.4	34.7	0.0	0.0	0.0	26.4	0.0
	3.27	Purple	286.2	0.0	56.7	38.6	37.1	0.0	0.0	9.6	0.0
	2.27	Red	1469.8	13.3	111.2	61.0	71.4	0.0	18.5	11.6	0.0
	1.27	Yellow	38321.2	180.4	2144.7	1177.4	2496.9	464.4	1108.4	1027.0	185.1
ML-12	5.27	Green	0.0	6.4	99.8	36.0	0.0	0.0	0.0	0.0	0.0
	4.27	Orange	0.0	15.2	206.0	84.3	0.0	4.4	0.0	0.0	0.0
	3.27	Purple	0.0	8.8	121.8	47.7	0.0	0.0	0.0	4.8	0.0
	2.27	Red	0.0	9.0	68.2	0.0	0.0	0.0	12.1	6.4	0.0
	1.27	Yellow	441.7	32.1	468.1	180.0	83.2	17.0	0.0	25.0	0.0

ML-13	4.27	Orange	329.2	12.7	150.6	72.8	58.2	0.0	8.4	8.1	0.0
	3.27	Purple	1252.6	21.0	300.4	133.8	97.3	19.7	44.2	36.2	0.0
	2.27	Red	0.0	12.9	36.0	0.0	0.0	0.0	9.6	0.0	0.0
	0.27	Clear	0.0	0.0	41.5	28.3	0.0	0.0	29.8	20.1	0.0
ML-14	4.27	Orange	0.0	0.0	0.0	0.0	0.0	0.0	0.0	0.0	0.0
	3.27	Purple	0.0	0.0	0.0	0.0	0.0	0.0	0.0	0.0	0.0
	1.27	Yellow	0.0	0.0	52.7	26.8	10.5	0.0	0.0	0.0	0.0
ML-16	2.27	Red	271.9	43.4	369.4	200.1	233.0	21.2	30.8	20.9	0.0
	1.27	Yellow	2674.7	85.3	524.6	242.8	200.0	28.8	42.2	36.6	0.0
	0.27	Clear	984.6	71.4	535.5	234.5	149.4	19.4	34.6	25.6	4.7
ML-17	1.27	Yellow	0.0	0.0	29.7	33.4	44.0	5.2	21.7	19.2	0.0
	0.27	Clear	0.0	10.2	128.2	99.4	162.9	17.5	26.1	24.0	0.0
ML-18	3.27	Purple	0.0	0.0	0.0	0.0	0.0	0.0	0.0	0.0	0.0
	2.27	Red	0.0	0.0	88.8	0.0	0.0	0.0	14.4	0.0	0.0
	1.27	Yellow	0.0	35.1	171.3	0.0	0.0	0.0	11.1	0.0	0.0
ML-20	3.27	Purple	0.0	0.0	0.0	0.0	0.0	0.0	0.0	0.0	0.0
	2.27	Red	0.0	0.0	0.0	0.0	0.0	0.0	0.0	0.0	0.0
	1.27	Yellow	0.0	0.0	0.0	0.0	0.0	0.0	0.0	0.0	0.0
	0.27	Clear	0.0	0.0	0.0	0.0	0.0	0.0	0.0	0.0	0.0
ML-21	3.27	Purple	0.0	0.0	0.0	0.0	0.0	0.0	0.0	0.0	0.0
	2.27	Red	0.0	0.0	0.0	0.0	0.0	0.0	0.0	0.0	0.0
	0.27	Clear	0.0	0.0	0.0	0.0	0.0	0.0	0.0	0.0	0.0

Table 4A: April 2000 Groundwater Data

MLS	Depth above Bedrock (ft)	Sampler	Napthalene ppb	Acenapthylene ppb	Acenapthene ppb	Fluorene ppb	Phenanthrene ppb	Anthracene ppb	Fluoranthene ppb	Pyrene ppb	Chrysene ppb
ML-1	7.27	Black	0.0	0.0	0.0	3.2	0.0	0.0	0.0	0.0	0.0
	6.27	Blue	0.0	0.0	0.0	0.0	0.0	0.0	0.0	0.0	0.0
	5.27	Green	0.0	0.0	0.0	3.1	0.0	0.0	0.0	0.0	0.0
	4.27	Orange	0.0	0.0	0.0	2.9	0.0	0.0	0.0	0.0	0.0
	3.27	Purple	0.0	0.0	4.2	3.4	0.0	0.0	0.0	0.0	0.0
	2.27	Red	0.0	0.0	5.0	3.2	0.0	0.0	0.0	0.0	0.0
	1.27	Yellow	0.0	0.0	6.1	3.6	0.0	0.0	0.0	0.0	0.0
	0.27	Clear	0.0	0.0	6.5	4.3	0.0	0.0	0.0	0.0	0.0
ML-3	7.27	Clear	0.0	0.0	0.0	3.0	0.0	0.0	0.0	0.0	0.0
	6.27	Blue	0.0	0.0	0.0	3.0	0.0	0.0	0.0	0.0	0.0
	5.27	Green	0.0	0.0	0.0	0.0	0.0	0.0	0.0	0.0	0.0
	4.27	Orange	0.0	0.0	0.0	2.7	0.0	0.0	0.0	0.0	0.0
	3.27	Purple	0.0	0.0	0.0	2.6	0.0	0.0	0.0	0.0	0.0
	2.27	Red	0.0	0.0	5.4	6.0	0.0	0.0	0.0	0.0	0.0
	1.27	Yellow	0.0	0.0	6.4	0.0	0.0	0.0	0.0	0.0	0.0
	0.27	Clear	0.0	0.0	20.5	12.6	12.9	0.0	7.7	0.0	0.0
ML-4	5.27	Green	0.0	0.0	0.0	0.0	0.0	0.0	0.0	0.0	0.0
	2.27	Red	105.0	21.4	167.4	86.7	158.5	19.4	34.7	24.7	0.0
	1.27	Yellow	0.0	18.0	120.6	69.1	56.8	16.7	22.9	16.6	0.0
	0.27	Clear	0.0	16.6	92.9	65.4	122.2	19.4	25.5	18.4	0.0
ML-5	6.27	Blue	0.0	0.0	0.0	0.0	0.0	0.0	0.0	0.0	0.0
	5.27	Green	0.0	0.0	0.0	0.0	0.0	0.0	0.0	0.0	0.0
	4.27	Orange	0.0	0.0	0.0	0.0	0.0	0.0	0.0	0.0	0.0
	3.27	Purple	0.0	0.0	0.0	0.0	0.0	0.0	0.0	0.0	0.0
	2.27	Red	0.0	0.0	0.0	0.0	0.0	0.0	0.0	0.0	0.0
	1.27	Yellow	0.0	0.0	0.0	0.0	0.0	0.0	0.0	0.0	0.0
	0.27	Clear	0.0	0.0	0.0	0.0	0.0	0.0	0.0	0.0	0.0
ML-7	5.27	Green	0.0	0.0	0.0	2.9	0.0	0.0	0.0	0.0	0.0
	4.27	Orange	5743.4	58.7	235.9	118.6	106.9	76.4	24.9	13.3	0.0
	3.27	Purple	5913.2	62.0	278.2	173.4	165.1	73.8	25.5	15.8	0.0
	2.27	Red	13823.3	132.5	538.5	286.1	282.0	133.7	40.1	28.8	0.0
ML-8	4.27	Orange	0.0	0.0	0.0	0.0	0.0	0.0	0.0	0.0	0.0
	3.27	Purple	442.3	21.6	99.5	37.2	28.7	10.4	9.1	8.0	0.0
	2.27	Red	111.6	0.0	27.0	14.8	17.3	0.0	0.0	0.0	0.0
	1.27	Yellow	0.0	0.0	13.1	7.1	8.0	0.0	0.0	0.0	0.0
	0.27	Clear	297.8	18.9	136.8	66.9	76.5	12.5	14.0	10.6	0.0
ML-9	2.27	Red	0.0	0.0	0.0	0.0	0.0	0.0	0.0	0.0	0.0
	1.27	Yellow	0.0	0.0	0.0	0.0	0.0	0.0	0.0	0.0	0.0

ML-10	4.27	Orange	0.0	0.0	0.0	0.0	0.0	0.0	0.0	0.0	0.0
	3.27	Purple	0.0	0.0	13.9	0.0	0.0	0.0	0.0	0.0	0.0
	2.27	Red	0.0	0.0	17.9	6.5	0.0	0.0	0.0	0.0	0.0
	1.27	Yellow	0.0	0.0	0.0	0.0	0.0	0.0	0.0	0.0	0.0
ML-11	4.27	Orange	49.4	15.2	32.8	16.6	5.3	0.0	0.0	6.6	0.0
	3.27	Purple	159.9	15.4	13.7	6.5	5.2	0.0	0.0	7.0	0.0
	2.27	Red	539.1	22.9	49.1	24.8	12.6	10.9	9.4	8.3	0.0
	0.27	Clear	14874.6	108.9	724.6	384.6	666.2	144.4	246.9	223.6	136.0
ML-12	5.27	Green	0.0	0.0	17.0	0.0	0.0	0.0	0.0	0.0	0.0
	4.27	Orange	0.0	0.0	8.9	0.0	0.0	0.0	0.0	0.0	0.0
	3.27	Purple	0.0	0.0	8.0	0.0	0.0	0.0	0.0	0.0	0.0
	2.27	Red	0.0	0.0	10.6	0.0	0.0	0.0	0.0	0.0	0.0
	1.27	Yellow	79.2	25.5	302.0	122.7	72.5	17.5	23.3	16.2	0.0
ML-13	5.27	Green	0.0	0.0	0.0	0.0	0.0	0.0	0.0	0.0	0.0
	4.27	Orange	0.0	0.0	5.9	0.0	0.0	0.0	0.0	0.0	0.0
	3.27	Purple	0.0	0.0	7.9	0.0	0.0	0.0	0.0	0.0	0.0
	2.27	Red	0.0	0.0	0.0	0.0	0.0	0.0	0.0	0.0	0.0
	1.27	Yellow	0.0	36.4	74.3	29.9	0.0	16.9	36.9	23.1	0.0
ML-14	6.27	Blue	0.0	0.0	0.0	0.0	0.0	0.0	0.0	0.0	0.0
	5.27	Green	0.0	0.0	0.0	0.0	0.0	0.0	0.0	0.0	0.0
	4.27	Orange	0.0	0.0	0.0	0.0	0.0	0.0	0.0	0.0	0.0
	3.27	Purple	0.0	0.0	0.0	0.0	0.0	0.0	0.0	0.0	0.0
	1.27	Yellow	0.0	0.0	12.0	5.6	0.0	0.0	0.0	0.0	0.0
ML-16	3.27	Purple	0.0	0.0	0.0	0.0	0.0	0.0	0.0	0.0	0.0
	2.27	Red	584.7	53.4	383.8	197.9	213.5	23.9	29.1	20.3	0.0
	1.27	Yellow	3046.2	87.7	567.8	263.3	248.8	24.6	32.2	24.9	0.0
	0.27	Clear	1333.5	74.7	582.5	260.1	222.2	22.8	33.7	24.6	0.0
ML-18	3.27	Purple	0.0	0.0	0.0	0.0	0.0	0.0	0.0	0.0	0.0
	2.27	Red	0.0	0.0	89.6	3.5	0.0	7.5	7.3	0.0	0.0
	1.27	Yellow	0.0	43.8	426.4	19.8	0.0	12.0	32.2	22.9	0.0
	0.27	Clear	315.4	43.9	516.0	232.4	133.7	29.1	38.1	28.8	0.0
ML-19	2.27	Red	0.0	0.0	0.0	0.0	0.0	0.0	0.0	0.0	0.0
	1.27	Yellow	0.0	0.0	0.0	0.0	0.0	0.0	0.0	0.0	0.0
	0.27	Clear	0.0	0.0	0.0	0.0	0.0	0.0	0.0	0.0	0.0
ML-22	3.27	Purple	0.0	0.0	48.8	30.6	14.7	13.8	24.5	17.3	0.0
	2.27	Red	0.0	24.7	145.1	98.8	103.8	18.6	22.2	16.1	0.0
ML-23	2.27	Red	0.0	0.0	13.1	27.4	174.8	22.1	48.2	33.7	0.0
	1.27	Yellow	0.0	0.0	27.8	41.3	156.2	19.8	42.7	30.3	0.0
ML-24	3.27	Purple	0.0	0.0	0.0	0.0	0.0	0.0	0.0	0.0	0.0
ML-25	3.27	Purple	0.0	0.0	0.0	0.0	0.0	0.0	0.0	0.0	0.0

Table 5A: Soil PAH Concentrations, July 1997.

Soil Bore ID	Depth BGS (ft)	Acenaphthene mg/kg	Fluorene mg/kg	Phenanthrene mg/kg	Fluoranthene mg/kg	Pyrene mg/kg	Chrysene mg/kg
SB1	3	0.43	1.73	2.69	10.15	13.29	21.56
	4	0.00	0.92	0.00	0.00	0.41	0.00
	5	0.08	1.11	0.00	0.00	0.83	0.00
	6	0.00	0.86	0.00	0.00	0.37	0.00
	7	0.00	1.07	0.00	0.00	0.51	0.00
	8	0.14	1.29	0.00	0.00	0.57	0.00
	8.167	0.13	1.02	0.58	2.14	2.07	0.00
SB2	4	0.17	0.18	0.00	0.00	0.39	0.00
	5	2.11	0.26	0.00	0.44	1.42	0.00
	6	0.00	0.00	0.12	0.21	0.00	0.00
	7	0.62	0.91	0.61	0.54	0.79	0.00
	8	1.06	1.55	1.59	1.00	0.81	0.00
SB3	3	2.28	3.06	4.77	22.84	23.52	24.81
	4	4.32	4.87	12.13	19.05	20.02	18.54
	5	55.87	71.28	281.70	271.60	259.20	128.30
	6	36.76	36.64	115.61	81.91	86.12	49.14
	7	2.80	2.70	7.57	20.31	18.77	7.27
	8	207.40	258.10	909.50	665.90	583.40	347.40
	9.833	184.38	181.70	565.55	329.78	229.57	157.53
SB4	3	0.00	0.00	0.00	0.00	0.00	0.00
	4	0.00	0.00	0.00	0.00	0.00	0.00
	5	0.00	0.20	0.00	0.00	0.35	0.00
	6	0.33	0.40	2.11	3.12	2.61	0.00
	7	14.26	21.35	89.89	61.50	53.11	20.18
	8	1.27	0.25	0.24	0.25	0.48	0.00
	9	0.81	0.66	2.19	2.05	1.79	0.40
	10	0.00	0.10	0.14	0.32	0.37	0.00
	10.833	10.23	7.59	3.95	4.62	3.43	0.00
SB6	4	0.00	0.00	0.00	0.00	0.00	0.00
	5.417	0.00	0.00	0.00	0.00	0.00	0.00
	6	0.00	0.00	0.00	0.00	0.00	0.00
	7	0.11	0.19	0.00	0.00	0.00	0.00
	8	0.00	0.00	0.18	0.00	0.10	0.00
	9	11.22	11.50	20.33	1.60	1.27	0.00

SB10	3	0.17	0.15	0.00	0.00	0.35	0.00
	4	0.00	0.14	0.00	0.00	0.33	0.00
	5	1.52	0.93	0.83	4.92	8.08	17.65
	6	470.34	553.00	1320.11	582.22	466.82	196.59
	7	644.71	721.16	1704.95	762.92	616.50	193.10
	8	473.60	510.80	1281.60	611.30	500.40	183.50
	9	204.48	209.86	596.76	317.97	222.88	87.84
	9.167	184.10	217.08	549.14	263.03	211.54	97.27
SB11	3	0.00	0.00	0.00	0.00	0.00	0.00
	4	0.00	0.00	0.00	0.00	0.00	0.00
	6	0.44	0.58	0.39	3.04	3.49	1.75
	7	3.30	6.77	29.70	19.92	16.45	5.04
	8	399.41	432.61	1119.61	583.20	488.28	166.34
SB12	3	0.00	0.15	0.00	0.18	0.49	0.00
	4	0.00	0.13	0.00	0.00	0.22	0.00
	5	0.00	0.16	0.00	0.00	0.39	0.00
	6	0.13	0.33	0.00	0.00	0.55	0.00
	7	0.00	0.31	0.00	0.00	0.44	0.00
	8	0.12	0.17	0.00	0.00	0.58	0.00
	9	2.04	1.66	0.29	0.00	1.70	0.00
	10	557.83	1019.09	3191.00	1635.52	1363.29	510.16
	10.25	17.01	42.09	161.43	82.73	82.73	47.93

Table 6A: Soil PAH Concentrations, October 1999.

Soil Bore ID	Depth BGS (ft)	Acenaphthene mg/kg	Fluorene mg/kg	Phenanthrene mg/kg	Fluoranthene mg/kg	Pyrene mg/kg	Chrysene mg/kg
SB1	3	1.89	3.19	5.06	11.30	14.54	15.07
	4	0.00	0.00	0.00	0.00	0.00	0.00
	5	0.00	0.00	0.00	0.00	0.00	0.00
	6	52.68	65.27	173.34	98.72	78.81	21.86
	7	0.00	0.00	0.00	0.00	0.00	0.00
	8	0.70	0.00	0.00	1.39	0.00	0.00
SB2	4	0.00	0.00	0.00	0.00	0.00	0.00
	5	0.00	0.89	0.00	0.00	0.00	0.00
	6	0.00	0.00	0.00	0.00	0.00	0.00
	7	0.00	0.00	0.00	0.00	0.00	0.00
	8	33.28	35.71	100.19	61.56	55.34	11.69
SB3	4.167	0.00	0.00	0.00	1.33	0.00	0.00
	5.167	0.00	0.75	0.00	4.97	4.17	3.08
	6.167	0.00	0.00	0.00	0.00	0.00	0.00
	7.167	0.79	0.00	1.59	0.00	0.00	0.00
	8.167	25.01	30.12	98.31	61.47	54.09	14.69
	8.833	184.91	194.91	573.21	323.96	278.49	81.57
SB4	3	0.00	0.00	0.00	0.00	0.00	0.00
	4	0.00	0.00	0.00	0.00	0.00	0.00
	5	0.00	0.00	0.00	0.00	0.00	0.00
	6	2.33	2.54	26.48	53.87	53.12	16.39
	7	16.16	24.03	91.77	53.12	45.97	11.72
	8	0.00	0.00	1.67	0.00	0.00	0.00
	9	0.00	0.00	1.08	0.00	0.00	0.00
	10	4.27	4.80	7.42	71.13	86.09	41.20
SB6	3	0.00	0.00	0.00	0.00	0.00	0.00
	4	0.00	0.00	0.00	0.00	0.00	0.00
	5	0.00	0.00	0.00	0.00	0.00	0.00
	6	0.00	0.00	0.00	0.00	0.00	0.00
	7	0.00	0.00	0.00	0.00	0.00	2.01
	8	0.00	0.00	0.00	0.00	0.00	2.01
	9	0.00	0.00	0.00	0.00	0.00	0.00
	10	4.44	3.99	6.93	1.65	0.00	0.00

SB10	2	0.00	0.00	0.00	0.00	0.00	0.00
	3	0.00	0.00	0.00	0.00	0.00	0.00
	4	1.55	1.87	4.18	11.60	9.08	10.44
	5	0.00	0.00	1.04	1.53	2.29	3.52
	6	142.23	187.86	466.86	208.69	167.88	46.66
	7	583.01	591.15	1542.48	617.95	514.22	130.05
	8	641.29	673.83	1746.34	807.27	684.47	202.30
	9	357.53	362.83	969.61	498.48	421.87	194.29
SB11	3	0.00	0.00	0.00	0.00	0.00	0.00
	4	0.00	0.00	0.00	0.00	0.00	2.06
	5	0.00	0.00	0.00	0.00	0.00	0.00
	6	0.00	0.00	0.00	0.00	0.00	0.00
	7	6.70	6.70	46.05	25.93	23.94	6.58
	8	597.07	597.07	1418.73	776.69	678.44	203.39
	9	1988.67	1988.67	5152.24	2676.13	2244.69	533.56
SB12	3	0.00	0.00	0.00	0.00	0.00	0.00
	4	0.00	0.00	0.00	0.00	0.00	0.00
	5	0.00	0.00	0.00	0.00	0.00	0.00
	6	0.00	0.00	0.00	0.00	0.00	0.00
	7	0.00	0.00	0.00	0.00	0.00	0.00
	8	0.00	0.00	0.00	0.00	0.00	0.00
	9	3.69	1.24	0.00	0.00	0.00	0.00
	10	712.03	638.30	1960.62	899.32	780.71	182.23

Table 7A: Dissolved Hydrogen in Groundwater Samples and Corresponding TEAP

MLS	Color	Hydrogen Conc (ppm)	Terminal Electron Acceptor Process (TEAP)
ML-1	Red	2.06	Sulfate-Reduction
ML-1	Red	0.64	Fe(III)-Reduction
ML-1	Yellow	0.98	Fe(III) or Sulfate-Reduction
ML-1	Yellow	0.84	Fe(III) or Sulfate-Reduction
ML-3	Yellow	1.46	Sulfate-Reduction
ML-3	Yellow	1.23	Sulfate-Reduction
ML-3	Yellow	2.11	Sulfate-Reduction
ML-3	Yellow	2.49	Sulfate-Reduction
ML-3	Yellow	1.74	Sulfate-Reduction
ML-3	Yellow	2.37	Sulfate-Reduction
ML-3	Clear	11.40	Methanogenesis
ML-3	Clear	12.29	Methanogenesis
ML-4	Red	3.88	Sulfate-Reduction
ML-4	Red	4.61	Sulfate-Reduction
ML-8	Clear	3.23	Sulfate-Reduction
ML-8	Clear	2.96	Sulfate-Reduction
ML-12	Red	0.94	Fe(III) or Sulfate-Reduction
ML-12	Red	1.17	Fe(III) or Sulfate-Reduction
ML-12	Yellow	3.82	Sulfate-Reduction
ML-13	Purple	2.94	Sulfate-Reduction
ML-13	Purple	3.56	Sulfate-Reduction
ML-13	Yellow	0.63	Fe(III)-Reduction
ML-14	Red	15.08	Methanogenesis
ML-14	Red	18.31	Methanogenesis
ML-16	Red	2.63	Sulfate-Reduction
ML-16	Red	3.03	Sulfate-Reduction
ML-16	Yellow	4.14	Sulfate-Reduction
ML-16	Yellow	5.39	Sulfate-Reduction
ML-16	Clear	1.78	Sulfate-Reduction
ML-16	Clear	4.37	Sulfate-Reduction

VITA

Mark Elliott was born on June 2nd, 1975, in Wilmington, Delaware. He attended high school at State College Area High School in State College, Pennsylvania. In June 1993, he graduated and began attending Penn State University, University Park Campus. In May 1998, he graduated from Penn State with a B.S. in Civil Engineering. He began work on a Master's Degree in Environmental Enginnering at Virginia Polytechnic Institute and State University in August 1998.